NASA Technical Paper 1173

Noise Transmission Through Plates Into an Enclosure

Wayne B. McDonald, Rimas Vaicaitis,
and Michael K. Myers

MAY 1978

NASA

NASA Technical Paper 1173

Noise Transmission Through Plates Into an Enclosure

Wayne B. McDonald
The George Washington University
Joint Institute for Advancement of Flight Sciences
Langley Research Center, Hampton, Virginia

Rimas Vaicaitis
Langley Research Center, Hampton, Virginia

Michael K. Myers
The George Washington University
Joint Institute for Advancement of Flight Sciences
Langley Research Center, Hampton. Virginia

NASA
National Aeronautics
and Space Administration

Scientific and Technical
Information Office

1978

SUMMARY

An analytical model is presented to predict noise transmission through elastic plates into a hard-walled rectangular cavity at low frequencies, that is, frequencies up through the first few plate and cavity natural frequencies. One or several nonoverlapping and independently vibrating panels are considered. The effects on noise transmission of different external pressure excitations, plate boundary conditions, fluid parameters, structural parameters, and geometrical parameters are investigated. Noise transmission is considerably affected by the specific form of external pressure loading. Raising plate natural frequencies results in less noise transmission below the fundamental plate natural frequency. If a single panel is replaced by several smaller panels, noise transmission is reduced below the fundamental natural frequency of the smaller panels but is not appreciably changed at higher frequencies.

INTRODUCTION

Sound inside an enclosure is frequently caused by external sources. External pressure fluctuations give rise to vibrations of the structure forming the enclosure and generate a sound field inside. For example, interior noise in aircraft is largely the result of sources which are external to the fuselage, such as engines or boundary-layer turbulence. Recent reports on general aviation, STOL, and turboprop aircraft indicate that such noise occurs primarily at low frequency (refs. 1 to 3). Also, noise in rooms of buildings may be caused by sources such as wind, cars, and airplanes. Analytical models capable of predicting the noise transmitted are essential to help determine those factors affecting transmission and to aid in the design of effective noise-reducing enclosures.

A great deal of information can be gained through a study of sound transmission through flexible walls into rigid cavities. For applications to aircraft interior noise it is important to include in an analytical model a representation of the actual construction of the vibrating surface. Aircraft sidewalls are generally composed of many individual panels stiffened by stringers and frames. In many cases these individual panels can be assumed to vibrate independently of each other, the total interior noise pressure being determined by superposition as if each panel were moving in an otherwise rigid wall. In a study of sound transmission into a rectangular cavity, for example, this behavior can be modeled by considering that only a portion of the vibrating wall is flexible.

A large volume of literature exists concerning noise transmission through panels into cavities, but only a small portion deals with the frequency range in which the first few panel and cavity resonances occur. References 4 to 14 describe sound transmission into rectangular enclosures with the whole of one wall flexible. Simply supported panels are treated in references 5 to 11, and

clamped panels are studied in references 12 to 14. However, it appears that no direct comparisons of the two panel support conditions have been made. Except for reference 8, previous work has been limited to cases in which the input pressure is uniform and fully correlated, and little is known about the effects of variations in the form of the external pressure field on the sound transmitted into the cavity.

The objective of the present work is to develop an analytical model to predict the noise transmitted through a rectangular elastic plate into an otherwise hard-walled cavity (see fig. 1). Particular attention is directed toward the low frequencies, that is, frequencies up through the first few plate and cavity resonances. The plate is driven by an external pressure which is assumed to be a random process, and the force exerted by the interior acoustic pressure on the plate is also taken into account. In the study, the plate displacement and the interior acoustic pressure are obtained in terms of the natural modes of the plate and cavity and are ultimately expressed in terms of spectral density functions. A quantity relating external pressure spectral density to the pressure spectral density at points inside the cavity is defined and called noise reduction.

The previous work cited has, in general, been directed toward a determination of the effect of the cavity on the response of the plate. The specific purpose of this paper, however, is to consider the nature of the sound field inside the cavity and to gain insight into how this field is affected by variations in several of the structural and input parameters. The major new analytic contribution here is the consideration of cases in which only a portion of one cavity wall is flexible. Nonoverlapping, independently vibrating panels can be treated by superposition of solutions for a single panel for applications to aircraft interior noise. Several such cases are discussed in this paper. The effect of three different external pressure excitations is investigated: a spatially uniform pressure, a spatially nonuniform pressure, and a turbulent boundary layer. In addition, noise transmission through both simply supported and clamped panels is treated, and comparisons are made to assess the influence of the plate support on the interior sound field. Finally, a comparison of the theoretical predictions with data obtained from a recent experiment is presented.

SYMBOLS

a,b,d cavity dimensions in x-, y-, and z-directions, respectively, m

c speed of sound, m/sec

D plate flexural rigidity, N-m

E modulus of elasticity, N/m^2

$F(x_1,y_1,x_2,y_2)$ deterministic function in modulated random process

h plate thickness, m

$H_{ijk}(\omega)$ defined by equation (24)

$H_{mn}(\omega)$ defined by equation (19)

$J_{mn}(\omega)$ defined by equation (27)

ℓ_x, ℓ_y plate dimensions in x- and y-directions, respectively, m

L_{ijmn} defined by equation (23)

$NR(x,y,z,\omega)$ noise reduction, dB

OASPL overall sound pressure level, dB

$p(x,y,z,t)$ cavity acoustic pressure, N/m^2

$p^e(x,y,t)$ external pressure, N/m^2

$\bar{P}^c_{mn}(\omega)$ generalized cavity force

$\bar{P}^e_{mn}(\omega)$ generalized random external force

$\bar{q}_{mn}(\omega)$ generalized coordinates for plate deflection

$R_x(\xi), R_y(\eta)$ spatial correlation coefficients

$S(x,y,z,\omega)$ spectral density of cavity pressure, $(N/m^2)^2/Hz$

$S^e(\xi,\eta,\omega)$ cross spectral density of external random pressure, $(N/m^2)^2/Hz$

$\hat{S}^e(\omega)$ spectral density of external random pressure, $(N/m^2)^2/Hz$

$S_{mns\ell}(\omega)$ defined by equation (29)

t time, sec

$w(x,y,t)$ plate displacement, m

x,y,z Cartesian coordinates, m

x_0, y_0 distance of plate from x- and y-axes, respectively, m

$X_{ijk}(x,y,z)$ orthonormal eigenfunctions of cavity

α_{ijk} cavity modal damping coefficients

β equivalent viscous damping, $N\text{-}sec/m^3$

$\Delta(z)$ $= z - \frac{z^2}{2d}$, m

η $= y_2 - y_1$, m

ζ_{mn} panel modal damping coefficients

ν	Poisson's ratio
ξ	$= x_2 - x_1$, m
ρ	air density, kg/m^3
ρ_s	plate density, kg/m^3
$\psi_{mn}(x,y)$	orthonormal eigenfunctions of plate
ω	frequency, rad/sec
ω_{ijk}	natural frequency of cavity, rad/sec
ω_{mn}	natural frequency of plate, rad/sec

Subscripts:

i...n,p...s	summation indices

ANALYSIS

Acoustical Problem

Consider a hard-walled rectangular cavity occupying a volume $V = abd$ as shown in figure 1. The rectangular plate at $z = 0$ is elastic with dimensions $x_0 \leqq x \leqq x_0 + \ell_x$, $y_0 \leqq y \leqq y_0 + \ell_y$. The remaining walls are assumed to be rigid. Several flexible and nonoverlapping panels may be located at $z = 0$. For this case it is assumed that the motions of these panels are independent. The solution for interior cavity pressure is developed separately for each panel and the total pressure is determined from superposition of the contributions by each panel. If the acoustic medium in the cavity is taken to be at rest prior to the motions of the panel, the perturbation pressure inside the enclosure is determined from the linear acoustic wave equation

$$\nabla^2 p = \frac{1}{c^2}\frac{\partial^2 p}{\partial t^2} \tag{1}$$

where $\nabla^2 = \partial^2/\partial x^2 + \partial^2/\partial y^2 + \partial^2/\partial z^2$ and the boundary conditions which express continuity of normal velocity between the fluid and the walls are

$$\frac{\partial p}{\partial n} = 0 \tag{2}$$

on the rigid cavity walls at $x = 0,a$, $y = 0,b$, $z = d$, and

$$\frac{\partial p}{\partial z} = \rho g(x,y,t) \tag{3}$$

on $z = 0$. Here $\partial p/\partial n$ is the pressure derivative normal to the wall surface, and

$$g(x,y,t) = \begin{cases} -\ddot{w}(x,y,t) & \left(\begin{matrix} x_0 \leqq x \leqq x_0 + \ell_x \\ y_0 \leqq y \leqq y_0 + \ell_y \end{matrix}\right) \\ 0 & \text{(Otherwise)} \end{cases} \tag{4}$$

where w is the displacement of the flexible wall in the z-direction. The problem as posed here considers only one flexible panel. By properly adjusting x_0, y_0, ℓ_x, and ℓ_y, additional panels at $z = 0$ can be considered.

To solve equation (1), the pressure can be written in terms of the orthonormal cavity eigenfunctions corresponding to hard walls at $x = 0,a$ and $y = 0,b$ in the form

$$p(x,y,z,t) = \sum_{i=0}^{\infty} \sum_{j=0}^{\infty} \Phi_{ij}(z,t) \sqrt{d}\, X_{ij0}(x,y) \tag{5}$$

where

$$X_{ijk}(x,y,z) = \sqrt{\frac{e_i e_j e_k}{abd}} \cos \frac{i\pi x}{a} \cos \frac{j\pi y}{b} \cos \frac{k\pi z}{d} \tag{6}$$

and

$$e_i = \begin{cases} 1 & (i = 0) \\ 2 & (i \neq 0) \end{cases} \tag{7}$$

When the flexible panel motions are expanded in terms of these cavity eigenfunctions and orthogonality is used,

$$\rho g = \sum_{i=0}^{\infty} \sum_{j=0}^{\infty} G_{ij}(t) \sqrt{d}\, X_{ij0}(x,y) \tag{8}$$

where

$$G_{ij}(t) = \int_{x_0}^{x_0+\ell_x} \int_{y_0}^{y_0+\ell_y} - \rho\ddot{w} \sqrt{d}\, X_{ij0}(x,y)\, dx\, dy \tag{9}$$

Equation (3) demonstrates that the boundary conditions for the functions $\Phi_{ij}(z,t)$ on $z = 0$ are not homogeneous. A direct application of separation of variables will not work for Φ_{ij} and a different method needs to be adopted. The solution can be achieved by transforming the homogeneous differential equation with nonhomogeneous boundary conditions into a nonhomogeneous differential equation with homogeneous boundary conditions. Using equations (1) to (8) and the expressions

$$\left.\begin{aligned}\Phi_{ij}(z,t) &= \phi_{ij}(z,t) + \Delta(z)\ G_{ij}(t)\\ \Delta(z) &= z - \frac{z^2}{2d}\end{aligned}\right\} \tag{10}$$

where the ϕ_{ij} are the solutions of the associated homogeneous problem and $\Delta(z)$ is chosen to satisfy the given boundary conditions, gives a nonhomogeneous equation with homogeneous boundary conditions. The associated homogeneous boundary-value problem has a solution:

$$\phi_{ij}(z,t) = \sum_{k=0}^{\infty} C_{ijk}(t)\ \sqrt{ab}\ X_{00k}(z) \tag{11}$$

Then the sound pressure distribution inside the cavity can be obtained by combining equations (5), (10), and (11). The result is

$$p(x,y,z,t) = \sum_{i=0}^{\infty}\sum_{j=0}^{\infty}\sum_{k=0}^{\infty} C_{ijk}(t)\ X_{ijk}(x,y,z) + \sum_{i=0}^{\infty}\sum_{j=0}^{\infty} \Delta(z)\ G_{ij}(t)\ \sqrt{d}\ X_{ij0}(x,y) \tag{12}$$

where the equation for the modal pressure coefficients is

$$\ddot{C}_{ijk} + 2\alpha_{ijk}\omega_{ijk}\dot{C}_{ijk} + \omega_{ijk}^2 C_{ijk} = F_{ijk}(t) \tag{13}$$

In equation (13) the damping in the cavity (wall absorption and viscous air damping) is included through the modal damping coefficients α_{ijk}. The cavity modal frequencies are

$$\omega_{ijk} = c\left[\left(\frac{i\pi}{a}\right)^2 + \left(\frac{j\pi}{b}\right)^2 + \left(\frac{k\pi}{d}\right)^2\right]^{1/2} \tag{14}$$

and the forcing function is

$$F_{ijk}(t) = \sqrt{ab}\int_0^d \left[\Delta(z)\ \ddot{G}_{ij} + \omega_{ij0}^2\ \Delta(z)\ G_{ij} - \frac{1}{c^2}\frac{d^2\Delta(z)}{dz^2}\ G_{ij}\right] X_{00k}(z)\ dz \tag{15}$$

The solution for the pressure coefficients C_{ijk} can be obtained by solving equation (13) in the time domain with specified initial conditions. However, for the noise-transmission study considered in this paper, it is more convenient to obtain the solution in the frequency domain. Hereinafter the solutions for the panel motions w and the cavity pressure p will be expressed in the frequency domain.

Plate Motion

For small deflections, the governing equation of motion for a panel located at $z = 0$ can be written in the frequency domain as

$$D\nabla^4\bar{w} + i\omega\beta\bar{w} - \rho_s h\omega^2\bar{w} = \bar{p}^e(x,y,\omega) - \bar{p}(x,y,0,\omega) \tag{16}$$

where $\nabla^4 = \partial^4/\partial x^4 + 2\partial^4/\partial x^2\partial y^2 + \partial^4/\partial y^4$, $D = Eh^3/12(1 - \nu^2)$, β is the viscous damping coefficient of the panel, $p^e(x,y,t)$ is the random external surface pressure, $p(x,y,0,t)$ is the cavity pressure at $z = 0$, and a bar indicates the Fourier transform. In the present analysis it is assumed that the viscous damping coefficient can be expressed as a linear combination of mass and stiffness so that the resulting modal equations will not be coupled through the structural damping term.

The solution for the plate deflection $\bar{w}$ is expressed in terms of normalized plate modes:

$$\bar{w} = \sum_{m=1}^{\infty}\sum_{n=1}^{\infty} \bar{q}_{mn}(\omega)\ \psi_{mn}(x,y) \tag{17}$$

where $\bar{q}_{mn}$ are the generalized coordinates and ψ_{mn} are the orthonormal plate modes. In the remainder of this work the indices m and n will be used to denote quantities related to the plate motion, and i,j,k will refer to the fluid motion. Substitution of equation (17) into equation (16) and utilization of the orthogonality principle gives

$$\bar{q}_{mn} = H_{mn}(\omega)\left[\bar{p}^e_{mn} - \bar{p}^c_{mn}(\bar{q}_{mn})\right] \tag{18}$$

where the frequency response function of the panel is

$$H_{mn}(\omega) = (\omega^2_{mn} - \omega^2 + 2i\zeta_{mn}\omega_{mn}\omega)^{-1} \tag{19}$$

and the generalized external and cavity forces are, respectively,

$$\bar{p}^e_{mn}(\omega) = \frac{1}{\rho_s h}\int_{x_0}^{x_0+\ell_x}\int_{y_0}^{y_0+\ell_y} \bar{p}^e(x,y,\omega)\ \psi_{mn}(x,y)\ dx\ dy \tag{20}$$

$$\bar{p}^c_{mn}(\omega) = \frac{1}{\rho_s h}\int_{x_0}^{x_0+\ell_x}\int_{y_0}^{y_0+\ell_y} \bar{p}(x,y,0,\omega)\ \psi_{mn}(x,y)\ dx\ dy \tag{21}$$

In equation (19), ω_{mn} and ζ_{mn} are the panel modal frequencies and panel modal damping coefficients, respectively. The generalized panel vibration coordinates $\bar{q}_{mn}$ are coupled through the generalized cavity force $\bar{p}^c_{mn}$. From equations (12), (13), (17), and (21),

$$\bar{p}^c_{mn} = \frac{\rho\omega^2}{\rho_s h}\sum_{i=0}^{\infty}\sum_{j=0}^{\infty}\sum_{k=0}^{\infty} H_{ijk}\sum_{r=1}^{\infty}\sum_{s=1}^{\infty} \bar{q}_{rs}L_{ijmn}L_{ijrs} \tag{22}$$

where

$$L_{ijmn} = \int_{x_0}^{x_0+\ell_x} \int_{y_0}^{y_0+\ell_y} \sqrt{d}\ X_{ij0}(x,y)\ \psi_{mn}(x,y)\ dx\ dy \tag{23}$$

and, for $\Delta(z) = z - z^2/2d$,

$$H_{ijk}(\omega) = \frac{-1}{\omega_{ijk}^2 - \omega^2 + 2i\alpha_{ijk}\omega_{ijk}\omega} \begin{Bmatrix} \frac{d}{3}\left(-\omega^2 + \omega_{ij0}^2 + \frac{3c^2}{d^2}\right) & (k = 0) \\ \frac{-d}{2(k\pi)^2}(\omega_{ij0}^2 - \omega^2) & (k \neq 0) \end{Bmatrix} \tag{24}$$

Combining equations (18) and (22) results in a system of coupled linear algebraic equations for the determination of $\bar{q}_{mn}$ in the form

$$\bar{q}_{mn} = H_{mn}\left(\bar{P}_{mn}^{e} - \frac{\rho\omega^2}{\rho_s h} \sum_{i=0}^{\infty} \sum_{j=0}^{\infty} \sum_{k=0}^{\infty} H_{ijk} \sum_{r=1}^{\infty} \sum_{s=1}^{\infty} \bar{q}_{rs} L_{ijmn} L_{ijrs}\right) \tag{25}$$

The final step to determine completely the plate motion and the acoustic field inside the cavity consists of solving the coupled system of equations (25) for $\bar{q}_{mn}$. It should be noted that equation (25) is completely general and accounts for all coupling effects between the plate and the cavity. The functions $H_{ijk}(\omega)$ and $H_{mn}(\omega)$ are the frequency response functions of the cavity and plate, respectively, and the quantities L_{ijmn} of equation (23) are the parameters which couple the plate vibration modes with the acoustic modes of the cavity. In the following section certain simplifying assumptions will be introduced in equation (25) in order to determine explicit approximate expressions for $\bar{q}_{mn}$ in terms of $\bar{P}_{mn}^{e}$.

Interior Acoustic Pressure

Simplifying assumptions.- The equations developed in the previous sections can be combined to construct a noise transmission model for elastic flexible panels. However, some simplifying assumptions have been suggested by previous work (refs. 5, 6, and 12 to 14) which can circumvent the lengthy numerical solution of the coupled system for $\bar{q}_{mn}$. The product $L_{ijmn}L_{ijrs}$ in equation (25) represents acoustic stiffness coupling between the plate mode mn and the plate mode rs through the fluid motion in the cavity at $z = 0$ (mode ij). The terms in equation (25) for which $r = m$, $s = n$ are called the direct acoustic stiffness, and those for which $r \neq m$, $s \neq n$ are termed the cross acoustic stiffness (ref. 5). It has been shown in the cited references that except when the panels are very thin and the cavities very shallow, the cross acoustic stiffness terms in equation (25) are negligible compared with the direct terms. Then equation (25) can be approximated by including only the terms $r = m$, $s = n$ in the summation, thus allowing an explicit expression for $\bar{q}_{mn}$ in terms of $\bar{P}_{mn}^{e}$ to be derived. Furthermore, provided that the plate itself is sufficiently

stiff, the direct acoustic stiffness is quite accurately modeled by assuming it affects only the fundamental plate mode (ref. 5).

In the results which follow it is assumed that the cavity is sufficiently deep and the plate sufficiently stiff that the approximations discussed above are valid. In this case, only the term $m = r = 1$, $n = s = 1$ on the right side of equation (25) is retained in the computation of $\bar{q}_{mn}$. Then, from equations (12) and (18) the acoustic pressure inside the enclosure is

$$\bar{p}(x,y,z,\omega) = \rho\omega^2 \sum_{i=0}^{\infty}\sum_{j=0}^{\infty}\left\{\left[\Delta(z) + \sum_{k=0}^{\infty}\sqrt{abd}\, H_{ijk}(\omega)\, X_{00k}(z)\right] \times \sum_{m=1}^{\infty}\sum_{n=1}^{\infty} J_{mn}(\omega)\, \bar{p}^{e}_{mn}(\omega)\, L_{ijmn}\right\}\sqrt{d}\, X_{ij0}(x,y) \tag{26}$$

where the frequency response function is

$$J_{mn}(\omega) = \begin{cases}\left[\omega_{11}^2 - \omega^2 + 2i\zeta_{11}\omega_{11}\omega + \dfrac{\rho\omega^2}{\rho_s h}\displaystyle\sum_{i=0}^{\infty}\sum_{j=0}^{\infty}\sum_{k=0}^{\infty} H_{ijk}L_{ij11}^2\right]^{-1} & (m = n = 1) \\ \left[\omega_{mn}^2 - \omega^2 + 2i\zeta_{mn}\omega_{mn}\omega\right]^{-1} & (\text{Otherwise})\end{cases} \tag{27}$$

Random analysis.- When the external input pressure p^e is random, statistical information on cavity pressure p in the form of spectral density and root-mean-square pressure is desired. The input pressure is assumed to be stationary and statistically homogeneous. However, numerical results are also presented for a special case of a nonhomogeneous process, in which a homogeneous random process is multiplied by a deterministic slowly varying function. Such a process is called a uniformly modulated random process and is very useful for practical applications (ref. 15). The cross spectral density of the cavity pressure $S(x_1,x_2;y_1,y_2;z_1,z_2;\omega)$ can be obtained by taking the mathematical expectation of equation (26) and following the procedure presented in reference 16. By setting $x_1 = x_2 = x$, $y_1 = y_2 = y$, $z_1 = z_2 = z$, the spectral density of the cavity pressure p is

$$S(x,y,z,\omega) = \rho^2\omega^4 \sum_{i=0}^{\infty}\sum_{j=0}^{\infty}\sum_{p=0}^{\infty}\sum_{q=0}^{\infty}\left\{\left[\Delta(z) + \sum_{k=0}^{\infty}\sqrt{abd}H_{ijk}X_{00k}\right] \times \left[\Delta(z) + \sum_{r=0}^{\infty}\sqrt{abd}H^*_{pqr}X_{00r}\right] dX_{ij0}X_{pq0} \times \sum_{m=1}^{\infty}\sum_{n=1}^{\infty}\sum_{s=1}^{\infty}\sum_{\ell=1}^{\infty} J_{mn}J^*_{s\ell}S_{mns\ell}L_{ijmn}L_{pqs\ell}\right\} \tag{28}$$

where the cross spectral density of the generalized random input forces is

$$S_{mns\ell} = \frac{1}{(\rho_s h)^2} \int_{x_0}^{x_0+\ell_x} \int_{x_0}^{x_0+\ell_x} \int_{y_0}^{y_0+\ell_y} \int_{y_0}^{y_0+\ell_y} S^e(\xi,\eta,\omega)\ \psi_{mn}(x_1,y_1) \times \psi_{s\ell}(x_2,y_2)\ dx_1\ dx_2\ dy_1\ dy_2 \tag{29}$$

in which S^e is the cross spectral density of the random input pressure p^e and $\xi = x_2 - x_1$, $\eta = y_2 - y_1$. The asterisks in equation (28) denote complex conjugates. For a spatially modulated random process, S^e in equation (29) is replaced by $\tilde{S}^e$, where

$$\tilde{S}^e(\xi,\eta,\omega) = S^e(\xi,\eta,\omega)\ F(x_1,y_1,x_2,y_2) \tag{30}$$

In equation (30), F is a deterministic function which varies slowly with x and y in comparison with random variations in $\bar{p}^e(x,y,\omega)$. For the numerical examples considered in this paper it was assumed that

$$S^e(\xi,\eta,\omega) = \hat{S}^e(\omega)\ R_x(\xi)\ R_y(\eta) \tag{31}$$

where $\hat{S}^e(\omega)$ is the spectral density of input pressure fluctuations, and $R_x(\xi)$ and $R_y(\eta)$ are the spatial correlation coefficients corresponding to the x- and y-coordinates, respectively.

Noise-reduction function.- A quantity relating the spectral density of the cavity pressure $S(x,y,z,\omega)$ to the spectral density of the external pressure $S^e(\omega)$ is the noise reduction NR, which is defined as

$$NR(x,y,z,\omega) = 10 \log \frac{\hat{S}^e(\omega)}{S(x,y,z,\omega)} \tag{32}$$

The numerical results for NR are evaluated for simply supported and clamped panels. For clamped panels the approximate characteristic beam functions are used to represent the clamped-clamped panel modes (ref. 17). Expressions for L_{ijmn} corresponding to these boundary conditions are presented in appendix A. Analytical formulae for $S_{mns\ell}$ corresponding to a uniform input pressure distribution, a nonuniform distribution, and turbulent boundary-layer pressure are included in appendix B.

DISCUSSION AND NUMERICAL RESULTS

Preliminaries

Noise reduction NR as defined in equation (32) provides a measure of the amount of noise transmitted through the flexible wall to a point inside the cavity. In order to determine the effect of variations in the loading, structural, and geometric parameters, a computer program was developed to calculate NR. The basic material parameters used in the calculations were taken to represent air and aluminum as follows:

$c = 344$ m/sec

$\rho = 1.21$ kg/m^3

$\rho_s = 2700$ kg/m^3

$E = 71$ kN/m^2

$\nu = 0.3$

Damping in the plate and cavity generally affects noise transmission only near plate and cavity resonant frequencies. Previous investigations (refs. 8 and 14) have considered in detail the increase in noise reduction near resonances which accompanies an increase in α_{ijk} or ζ_{mn}. They conclude, for example, that a doubling of either α_{ijk} or ζ_{mn} yields a maximum of 6-dB more noise reduction at resonances. This conclusion is supported by calculations based on the present theory. However, for the results presented here both α_{ijk} and ζ_{mn} were set equal to 0.02 on the basis of a comparison with an experimental measurement of noise reduction presented in this discussion.

An investigation of the convergence of the various series involved in the calculation of noise reduction indicated that it was necessary to include enough structural modes (indices m and n) to cover all structural natural frequencies in the frequency range of interest (0 to 1000 Hz). Since the structural modes are expanded in terms of the acoustic modes at $z = 0$ (indices i and j), it was necessary to include more acoustic than structural modes. In all cases studied it was found sufficient for numerical convergence to include acoustic modes for which i and j go to values 3 higher than m and n, and k goes to 5.

Previous results (ref. 18) have indicated that for systems which are lightly damped or are subjected to relatively smooth excitation cross spectral densities, the cross terms $i \neq p$, $j \neq q$, $k \neq r$, $m \neq s$, $n \neq \ell$ in equation (28) are negligible compared with the joint terms $i = p$, $j = q$, $k = r$, $m = s$, $n = \ell$. Figure 2 gives a sample of calculations made to verify that this is true for the present problem. The particular case shown corresponds to a spatially uniform external pressure spectral density ($R_x = R_y = 1$ in eq. (31)). The noise reduction NR is computed at the point $x = 0.1524$ m, $y = 0.2032$ m, $z = 0$ m for a cavity of dimensions $a = 0.4572$ m, $b = 0.6096$ m, $d = 0.9144$ m. The panel has dimensions $\ell_x = 0.2639$ m, $\ell_y = 0.3520$ m, $h = 0.001524$ m and is located such that $x_0 = 0.0965$ m and $y_0 = 0.0129$ m. Its edges are assumed clamped. Virtually no difference is observed near the natural frequencies of the panel and cavity if the cross terms are omitted from equation (28), and a difference of no more than 2 or 3 dB is seen in the intervals between these frequencies. Also, noise reduction is underestimated by neglecting these terms. Thus, in order to minimize computation time, all results for noise reduction presented in the remaining figures were calculated by omitting the cross terms in equation (28).

It is of interest to consider briefly the limiting case of very low frequency. It can be shown that as ω tends toward zero, all the terms having nonzero indices i, j, k, p, q, r in equation (28) vanish, yielding

$$\lim_{\omega \to 0} S(x,y,z,\omega) = \sum_{m=1}^{\infty} \sum_{n=1}^{\infty} \left| J_{mn}^{0} \right|^{2} S_{mnmn} L_{00mn}^{2}$$

where

$$\left| J_{mn}^{0} \right|^{2} = \begin{cases} \left(\omega_{11}^{2} + \dfrac{\rho c^{2}}{\rho_{s} h} L_{0011}^{2} \right)^{-1} & (m = n = 1) \\ \omega_{mn}^{-2} & (\text{Otherwise}) \end{cases}$$

under the assumption, as discussed in the preceding paragraph, that the cross terms in equation (28) can be ignored. If the double sum above is approximated by the leading term $m = n = 1$, then

$$NR = 10 \log \frac{\omega_{11}^{2} + \dfrac{\rho c^{2}}{\rho_{s} h} L_{0011}^{2}}{S_{1111} L_{0011}^{2}}$$

This expression reduces to the one obtained by Lyon (ref. 4) using a static analysis for a cavity with one whole wall flexible. It was found to approximate closely the numerically computed results of equation (28) so long as the frequency ω remains below the lowest natural frequencies of the cavity and panel.

The effect on NR of the fluid density ρ is easily seen from equation (28). It affects NR primarily as a multiplier outside the entire series. Hence, NR is nearly proportional to $-20 \log \rho$, and doubling ρ decreases NR by 6 dB at all frequencies.

Prior to discussion of the remaining figures, it should be mentioned that in each (including fig. 2) certain panel and cavity resonant frequencies are indicated. There are numerous cavity resonances in the frequency range covered by the various figures. Whenever one of these cavity resonances is excited by the panel motion at the particular calculation point considered, it is indicated by a solid circular symbol below the resulting local minimum of NR. Those cavity resonances which are not excited by the panel or which yield an insignificant drop in NR are not indicated in the figures.

Effects of Different External Pressure Distributions

In order to compute noise reduction NR from equation (32), an explicit form for the external pressure cross spectral density S^{e} must be specified. Three different forms are considered here: a spatially uniform pressure, a spatially nonuniform pressure, and a turbulent boundary-layer excitation. The specific expressions for $S_{mns\ell}$ in these instances are given in appendix B. Figures 3 and 4 present the results for the nonuniform and uniform distribution of pressure for simply supported panels. The cavity dimensions are $a = 0.4572$ m, $b = 0.6096$ m, $d = 0.9144$ m, and the plate thickness h is 0.001524 m.

Figure 3 depicts the noise reduction calculated at the point $x = 0.1524$ m, $y = 0.2032$ m, $z = 0.3048$ m for a flexible surface consisting of four nonoverlapping equal size panels, each simply supported on its edges. Because of the sinusoidal variation chosen for the nonuniform external pressure, only the fundamental mode of each panel is excited in the nonuniform case. The figure illustrates the fact that the spatially nonuniform pressure yields more noise reduction at all frequencies for this configuration.

In figure 4, the same cavity, calculation position, and panel thickness are used, but a single simply supported panel is considered. The panel is located at $x_0 = 0.0762$ m, $y_0 = 0.127$ m and is of dimensions $\ell_x = 0.254$ m and $\ell_y = 0.2794$ m. In this case all structural modes are excited. It is seen from figure 4 that at low frequencies, the noise reduction is significantly higher for the nonuniform pressure than for the uniform pressure. However this does not hold true as the frequency increases. For the single panel, very little increase in noise reduction is obtained for the nonuniform pressure as the frequency increases, and at some of the higher panel natural frequencies the noise reduction is less for the nonuniform than for the uniform pressure. The large decrease at 410 Hz occurs because an acoustic mode and a panel mode have about the same natural frequencies.

The third type of external pressure distribution to be considered is turbulent boundary-layer noise. The specific form of the correlation functions used is given in appendix B. Figure 5 presents the noise reduction for partially correlated and fully correlated noise ($R_x = R_y = 1$). For this figure the cavity is of dimensions $a = 0.2032$ m, $b = 0.4064$ m, $d = 0.6096$ m, and the simply supported panel occupies the entire wall $z = 0$. The panel thickness is again taken to be 0.001524 m. It is seen from figure 5 that at all frequencies, the fully correlated noise provides much less noise reduction, generally about 12 to 15 dB less, than the partially correlated noise.

The results of figures 3, 4, and 5 indicate that in general the specific form of the external pressure distribution can alter significantly the noise-reduction characteristics of the structure and cavity and should be considered along with the structural and material parameters in any discussion of sound transmission into the cavity. However, for the remainder of the results to be presented, only the spatially uniform distribution will be used.

Effects of Varying Structural Parameters

The plate density ρ_s appears as a multiplier in equation (29) for $S_{mns\ell}$ and therefore as a multiplier in equation (28) for S. Thus NR (eq. (32)) is proportional to $20 \log \rho_s$, and doubling ρ_s would give a 6-dB increase in NR. However, the density also appears in conjunction with the other two material parameters E and ν in the plate natural frequencies ω_{mn}. The effect of variations of these frequencies and of other structural parameters is illustrated in figures 6, 7, and 8. All describe a cavity of dimensions $a = 0.4572$ m, $b = 0.6096$ m, $d = 0.9144$ m and a panel with $\ell_x = 0.2639$ m, $\ell_y = 0.352$ m located at $x_0 = 0.0965$ m, $y_0 = 0.1285$ m. The point at which the noise reduction is calculated is $x = 0.1524$ m, $y = 0.2032$ m, $z = 0.3048$ m.

In figure 6 the effect of doubling panel natural frequencies for a clamped panel of thickness 0.001524 m is shown. As could be expected from the low-frequency approximation given earlier in this section, noise reduction is increased by doubling ω_{mn} at the lower frequencies. It is not altered significantly at higher frequencies except near the panel resonances. It should be noted that, because ω_{mn} is proportional to $\rho_s^{-1/2}$, increasing ρ_s will decrease noise reduction at low frequency, tending to counteract the effect from $S_{mns\ell}$.

The effect of increasing the thickness of a clamped panel appears in figure 7. The cross spectral density of the generalized random input forces $S_{mns\ell}$ is proportional to h^{-2} and ω_{mn} is proportional to h. Hence, a doubling of h will increase noise reduction by more than 6 dB at low frequencies. The figure presents noise reduction for panels of thicknesses h = 0.001016, 0.001778, and 0.00254 m over the frequency range 0 to 1200 Hz. For the intermediate thickness the acoustic natural frequency ω_{001} and the structural natural frequency ω_{11} are nearly equal. This combined resonance produces a large amplification of sound near this frequency (about 180 Hz).

The remaining structural parameter of interest is the support condition itself. The noise reduction for simply supported and clamped panels is shown in figure 8 for the same cavity and panel as in figure 6. At higher frequencies both conditions provide about the same amount of noise reduction except near the panel natural frequencies. At resonance, the clamped-edge panel always gives less noise reduction than does the simply supported panel. As the frequency becomes small, however, the clamped panel provides more noise reduction, since its fundamental resonant frequency is higher than that of the simply supported panel.

Effects of Varying Geometric Parameters

All the remaining figures refer to panels having clamped edges and thickness h = 0.001524 m. Figures 9, 10, and 11 refer to the same cavity used in the previous three figures and a calculation point for noise reduction at x = 0.1524 m, y = 0.2032 m, z = 0.3048 m. Figure 9 is obtained by varying the position on the wall z = 0 of a panel having ℓ_x = 0.1016 m, ℓ_y = 0.1524 m. A difference of 0 to 4 dB in noise reduction is observed for the two panel positions over the entire frequency range. As might be anticipated, the smallest noise reduction is obtained when the panel is located over the point at which the noise reduction is calculated. Figure 10 shows the effect at the same point in the cavity of varying the size of the panel. Generally, noise reduction is increased by using smaller panels.

Results for a single panel occupying the entire wall z = 0 and four equal size panels occupying the same wall are shown in figure 11. For frequencies below the fundamental natural frequency of the small panels, the multiple-panel configuration results in a larger noise reduction than does the single panel. This occurs primarily because of the effective increase in stiffness associated with the multiple panels. At higher frequencies the noise reduction is about the same for both configurations. Similar results have been obtained for other multiple-panel configurations.

Figure 12 refers to a panel for which $\ell_x = 0.4572$ m, $\ell_y = 0.6096$ m, located over three different sized cavities for which the ratio a:b:d is held as 3:4:6. The position for calculation of noise reduction is maintained so that the x,y location is the same in each case with respect to the panel, and the ratio z/d is held fixed. For the entire range of frequencies, noise reduction is generally higher for larger boxes. Small variations in this pattern occur, no doubt as a result of the fact that the natural frequencies of the cavities differ and thus they interact with the panel motion differently. It should be noted, however, that the position at which noise reduction is calculated in the cavity is important in this case. Variations in noise reduction at different depths below $z = 0$ or because of differences in relative position of panel and calculation point can produce results quite unlike those of figure 12.

The remaining illustrations of geometric effects on noise reduction are contained in figures 13, 14, and 15. All these figures describe the same cavity and clamped panel as in figures 6, 7, and 8 (see the previous section) and illustrate the variation of interior noise with position in the cavity. In figure 13, noise reduction is calculated at $x = 0.1524$ m, $y = 0.2032$ m at both $z = 0$ and $z = 0.4064$ m. For frequencies below the first structural natural frequency, the noise reduction is about the same at each depth below the panel. As the frequency increases, the noise reduction becomes 12 to 15 dB higher at the point farther below the panel.

Figure 14(a) shows OASPL, defined over the frequency range f_1 to f_2 by

$$\mathrm{OASPL} = 10 \log \frac{\int_{f_1}^{f_2} S(x,y,z,\omega)\, d\omega}{p_{ref}^2}$$

(where $p_{ref} = 20\ \mu N/m^2$) at the same x,y position used in figure 13 as a function of distance below the panel for $S^e(\omega) = 6.366\ (N/m^2)^2/Hz$. About a 12-dB variation is seen, the minimum OASPL occurring near the midheight of the cavity. Figure 14(b) shows OASPL at $y = 0.2032$ m as a function of x at a given $z = 0.3048$ m. As seen from these two figures, the variation in noise reduction parallel to the panel is much smaller (<3 dB across the width) than the variation normal to the panel. This is also seen in figure 15, which shows noise reduction at $x = 0$ and $x = 0.3048$ m.

Comparison of Theoretical and Experimental Results

Finally, noise reduction values predicted by equation (32) were compared with experimental values measured at a single point $x = 0.1594$ m, $y = 0.193$ m, $z = 0.127$ m in a cavity of dimensions $a = 0.3099$ m, $b = 0.386$ m, $d = 0.4572$ m. (The experimental values, as yet unpublished, were obtained by C. Kearney Barton, of Langley Research Center.) The external-pressure excitation used was spatially uniform white noise at a level of 100 dB, and the panel occupied the entire face $z = 0$ of the cavity. Figure 16 shows calculated and measured

narrow-band noise reduction; figure 17 depicts the same results for 1/3-octave band noise reduction obtained from

$$(NR)_{1/3} = 10 \log \frac{\int_{f_\ell}^{f_u} \hat{S}^e(\omega)\, d\omega}{\int_{f_\ell}^{f_u} S(x,y,z,\omega)\, d\omega}$$

in which f_ℓ and f_u are the lower and upper limits of the 1/3-octave bands.

CONCLUDING REMARKS

This paper presents an analytical model to predict noise transmission through elastic plates into a hard-walled rectangular cavity for frequencies through the first few plate and cavity resonant frequencies. Unlike previous work which assumes the whole of one wall to be flexible, this study treats cases in which the plate occupies only a portion of the wall. Several nonoverlapping plates are considered by assuming the motion of each plate to be independent of the others and using superposition to obtain the total cavity pressure. An external pressure that is assumed to be a random process excites the plate vibrations. An expression is obtained for the spectral density of the cavity acoustic pressure in terms of the natural modes of the plate and cavity. An expression is also obtained for the primary quantity of interest here, noise reduction, which relates the external pressure spectral density to the cavity pressure spectral density. It provides a measure of the amount that the external noise has been reduced in being transmitted through the panel into the cavity.

To determine their effect on noise reduction, different external pressure distributions and plate boundary conditions are used and some of the fluid, structural, and geometric parameters are varied. From the results obtained, the following generalizations are made:

1. External pressure distribution - The specific form of the external loading can have a considerable effect on noise reduction.

2. Plate boundary conditions - A clamped-edge plate gives more noise reduction below its fundamental natural frequency than a simply supported one. However, the noise reduction is about the same at higher frequencies, except that at plate natural frequencies the clamped-edge plate yields less noise reduction.

3. Fluid parameters - Increased acoustic damping can increase noise reduction at cavity natural frequencies. If the fluid density is doubled, noise reduction is decreased by 6 dB.

4. Structural parameters - Increased structural damping increases noise reduction at panel natural frequencies. Increasing the panel natural frequencies increases noise reduction. In addition, doubling plate material density or thickness increases noise reduction by 6 dB.

5. Geometrical parameters - Smaller panels in general yield more noise reduction. Replacing one panel by several smaller panels increases noise reduction below and near the fundamental natural frequency of the smaller panels, but has little effect on noise reduction at higher frequencies. Considerable variation of noise reduction in the direction normal to the plane of the plate is observed.

Langley Research Center
National Aeronautics and Space Administration
Hampton, VA 23665
March 14, 1978

APPENDIX A

EVALUATION OF L_{ijmn}

The quantity L_{ijmn} in equation (23) is evaluated for both simply supported and clamped panels. The modes used for the simply supported panel are

$$\psi_{mn}(x,y) = \frac{2}{\sqrt{\ell_x \ell_y}} \sin \frac{m\pi}{\ell_x}(x - x_0) \sin \frac{n\pi}{\ell_y}(y - y_0)$$

For the clamped panel a rough approximation for the modes can be obtained by using clamped-beam modes in the form (ref. 17)

$$\psi_{mn}(x,y) = \psi_m'(x;x_0)\ \psi_n'(y;y_0)$$

where

$$\psi_m'(x;x_0) = \frac{1}{A_m\sqrt{\ell_x}}\begin{cases} \cos \gamma_m\left(\dfrac{x - x_0}{\ell_x} - \dfrac{1}{2}\right) + \kappa_m \cosh \gamma_m\left(\dfrac{x - x_0}{\ell_x} - \dfrac{1}{2}\right) & (m \text{ odd}) \\ \sin \gamma_m\left(\dfrac{x - x_0}{\ell_x} - \dfrac{1}{2}\right) + \kappa_m \sinh \gamma_m\left(\dfrac{x - x_0}{\ell_x} - \dfrac{1}{2}\right) & (m \text{ even}) \end{cases}$$

The values of the constants A_m, γ_m, and κ_m from reference 17 are given in table A1.

TABLE A1.- CONSTANTS FOR CLAMPED-PLATE MODES

m	A_m	γ_m	κ_m	α_m
1	0.7133	4.730040	0.132857	0.982
2	.7068	7.853202	-.0278749	1.00
3	.7071	10.995608	-.00579227	1.00
4	.7071	14.137164	.0012041	1.00
5	.7071	17.278758	.002503	1.00
>5	.7071	$\gamma_5 + (m - 5)\pi$	$\dfrac{\sin \frac{\gamma_m}{2}}{\sinh \frac{\gamma_m}{2}}$	1.00

APPENDIX A

For the simply supported panel, L_{ijmn} defined by equation (23) is given by

$$L_{ijmn} = L(i,m,x_0,\ell_x,a)\ L(j,n,y_0,\ell_y,b)$$

where

$$L(i,m,x_0,\ell_x,a) = \begin{cases} \sqrt{\dfrac{2}{a\ell_x}}\ \dfrac{\ell_x}{m\pi}\left[1 - (-1)^m\right] & (i = 0) \\[2ex] \dfrac{-\ell_x}{\sqrt{a\ell_x}}\ \sin\dfrac{m\pi x_0}{\ell_x} & \left(\dfrac{i\pi}{a} = \dfrac{m\pi}{\ell_x}\right) \\[2ex] \dfrac{2}{\sqrt{a\ell_x}}\ \dfrac{m\pi}{\ell_x}\ \dfrac{\cos\dfrac{i\pi x_0}{a} - (-1)^m \cos\dfrac{i\pi}{a}(x_0 + \ell_x)}{(m\pi/\ell_x)^2 - (i\pi/a)^2} & \left(\dfrac{i\pi}{a} \neq \dfrac{m\pi}{\ell_x}\right) \end{cases}$$

For the clamped panel, L_{ijmn} becomes

$$L_{ijmn} = \left[I_1(i,m,x_0,\ell_x,a) + \kappa_m I_2(i,m,x_0,\ell_x,a)\right]\left[I_1(j,n,y_0,\ell_y,b) + \kappa_n I_2(j,n,y_0,\ell_y,b)\right]$$

where, for m odd,

$$I_1(i,m,x_0,\ell_x,a) = \begin{cases} \dfrac{1}{A_m}\sqrt{\dfrac{\ell_x}{a}}\ \dfrac{\sin\dfrac{\gamma_m}{2}}{\dfrac{\gamma_m}{2}} & (i = 0) \\[3ex] \dfrac{1}{A_m}\sqrt{\dfrac{2\ell_x}{a}}\left[\cos\gamma_m\left(\dfrac{x_0}{\ell_x} + \dfrac{1}{2}\right) + \dfrac{1}{2\gamma_m}\sin\left(\dfrac{\gamma_m x_0}{\ell_x} + \dfrac{3\gamma_m}{2}\right)\right. \\ \left. - \dfrac{1}{2\gamma_m}\sin\left(\dfrac{\gamma_m x_0}{\ell_x} - \dfrac{\gamma_m}{2}\right)\right] & \left(\dfrac{\gamma_m}{\ell_x} = \dfrac{i\pi}{a}\right) \\[3ex] \dfrac{1}{A_m}\sqrt{\dfrac{2}{a\ell_x}}\left\{\dfrac{\sin\left[\dfrac{i\pi}{a}(x_0 + \ell_x) - \dfrac{\gamma_m}{2}\right] - \sin\left(\dfrac{i\pi x_0}{a} + \dfrac{\gamma_m}{2}\right)}{2\left(\dfrac{i\pi}{a} - \dfrac{\gamma_m}{\ell_x}\right)}\right. \\ \left. + \dfrac{\sin\left[\dfrac{i\pi}{a}(x_0 + \ell_x) + \dfrac{\gamma_m}{2}\right] - \sin\left(\dfrac{i\pi x_0}{a} - \dfrac{\gamma_m}{2}\right)}{2\left(\dfrac{i\pi}{a} + \dfrac{\gamma_m}{\ell_x}\right)}\right\} & \left(\dfrac{\gamma_m}{\ell_x} \neq \dfrac{i\pi}{a}\right) \end{cases}$$

and

$$I_2(i,m,x_0,\ell_x,a) = \begin{cases} \dfrac{1}{A_m\sqrt{a\ell_x}}\,\dfrac{2\ell_x}{\gamma_m}\sinh\dfrac{\gamma_m}{2} & (i = 0) \\[2ex] \dfrac{\dfrac{1}{A_m}\sqrt{\dfrac{2}{a\ell_x}}}{\left(\dfrac{\gamma_m}{\ell_x}\right)^2 + \left(\dfrac{i\pi}{a}\right)^2}\left\{\dfrac{\gamma_m}{\ell_x}\sinh\dfrac{\gamma_m}{2}\left[\cos\dfrac{i\pi}{a}(x_0 + \ell_x) + \cos\dfrac{i\pi x_0}{a}\right]\right. \\ \qquad\qquad \left. + \dfrac{i\pi}{a}\cosh\dfrac{\gamma_m}{2}\left[\sin\dfrac{i\pi}{a}(x_0 + \ell_x) - \sin\dfrac{i\pi x_0}{a}\right]\right\} & (i \neq 0) \end{cases}$$

For m even,

$$I_1(i,m,x_0,\ell_x,a) = \begin{cases} 0 & (i = 0) \\[2ex] -\dfrac{1}{A_m}\sqrt{\dfrac{\ell_x}{2a}}\sin\left(\dfrac{i\pi x_0}{a} + \dfrac{\gamma_m}{2}\right) - \dfrac{1}{4i\pi A_m}\sqrt{\dfrac{2a}{\ell_x}}\left[\cos\left(\dfrac{i\pi x_0}{a} + \dfrac{3\gamma_m}{2}\right)\right. \\ \qquad \left. - \cos\left(\dfrac{i\pi x_0}{a} - \dfrac{\gamma_m}{2}\right)\right] & \left(\dfrac{\gamma_m}{\ell_x} = \dfrac{i\pi}{a}\right) \\[2ex] -\dfrac{1}{A_m}\sqrt{\dfrac{2}{a\ell_x}}\left\{\dfrac{\cos\left[\dfrac{\gamma_m}{2} - \dfrac{i\pi}{a}(x_0 + \ell_x)\right] - \cos\left(\dfrac{i\pi x_0}{a} + \dfrac{\gamma_m}{2}\right)}{2\left(\dfrac{\gamma_m}{\ell_x} - \dfrac{i\pi}{a}\right)}\right. \\ \qquad \left. + \dfrac{\cos\left[\dfrac{i\pi}{a}(x_0 + \ell_x) + \dfrac{\gamma_m}{2}\right] - \cos\left(\dfrac{i\pi x_0}{a} - \dfrac{\gamma_m}{2}\right)}{2\left(\dfrac{\gamma_m}{\ell_x} + \dfrac{i\pi}{a}\right)}\right\} & \left(\dfrac{\gamma_m}{\ell_x} \neq \dfrac{i\pi}{a}\right) \end{cases}$$

and

$$I_2(i,m,x_0,\ell_x,a) = \begin{cases} 0 & (i = 0) \\ \dfrac{\dfrac{1}{A_m}\sqrt{\dfrac{2}{a\ell_x}}}{\left(\dfrac{\gamma_m}{\ell_x}\right)^2 + \left(\dfrac{i\pi}{a}\right)^2} \left\{\dfrac{\gamma_m}{\ell_x} \cosh \dfrac{\gamma_m}{2}\left[\cos \dfrac{i\pi}{a}(x_0 + \ell_x) - \cos \dfrac{i\pi x_0}{a}\right] \right. & \\ \qquad \left. + \dfrac{i\pi}{a} \sinh \dfrac{\gamma_m}{2}\left[\sin \dfrac{i\pi}{a}(x_0 + \ell_x) - \sin \dfrac{i\pi x_0}{a}\right]\right\} & (i \neq 0) \end{cases}$$

APPENDIX B

EVALUATION OF $S_{mns\ell}$

For a uniform pressure distribution $R_x = R_y = 1$ in equation (31), the quantity $S_{mns\ell}$ is calculated from equation (29) for a simply supported panel as

$$S_{mns\ell} = \frac{\hat{S}^e(\omega)}{\rho_s{}^2h^2}\,\frac{4\ell_x\ell_y}{mns\ell\pi^4}\left[1 - (-1)^m\right]\left[1 - (-1)^n\right]\left[1 - (-1)^s\right]\left[1 - (-1)^\ell\right]$$

For the clamped panel, using the approximate modes given in appendix A yields

$$S_{mns\ell} = \frac{\hat{S}^e(\omega)}{\rho_s{}^2h^2}\,\frac{16\ell_x\ell_y\alpha_m\alpha_n\alpha_s\alpha_\ell}{\gamma_m\gamma_n\gamma_s\gamma_\ell}\left[1 - (-1)^m\right]\left[1 - (-1)^n\right]\left[1 - (-1)^s\right]\left[1 - (-1)^\ell\right]$$

where the values for α_m and γ_m are given in table A1.

As a particular example of a nonuniform pressure distribution, it is assumed that the random input pressure is modulated by a sine function. Then in equation (30), F is chosen in the form

$$F = f(x_1/a)\ f(x_2/a)\ f(y_1/b)\ f(y_2/b)$$

where $f(x) = \sin(2\pi x)$. Then equation (29) gives, for a simply supported panel,

$$S_{mns\ell} = \frac{\hat{S}^e(\omega)}{\rho_s{}^2h^2}\ I(m,x_0,\ell_x,a)\ I(n,y_0,\ell_y,b)\ I(s,x_0,\ell_x,a)\ I(\ell,y_0,\ell_y,b)$$

where

$$I(m,x_0,\ell_x,a) = \begin{cases} \sqrt{\dfrac{\ell_x}{a}}\cos\dfrac{m\pi x_0}{\ell_x} & \left(\dfrac{2\pi}{a} = \dfrac{m\pi}{\ell_x}\right) \\[2ex] \sqrt{\dfrac{2}{\ell_x}}\,\dfrac{m\pi}{\ell_x}\,\dfrac{(-1)^m\sin\dfrac{2\pi}{a}(x_0 + \ell_x) - \sin\dfrac{2\pi x_0}{\ell_x}}{\left(\dfrac{2\pi}{a}\right)^2 - \left(\dfrac{m\pi}{\ell_x}\right)^2} & \left(\dfrac{2\pi}{a} \neq \dfrac{m\pi}{\ell_x}\right) \end{cases}$$

Similar expressions can be obtained for clamped boundary conditions. However, they are very lengthy and are not included here.

Consider the turbulent boundary-layer pressure fluctuations expressed in the form of equation (31). For a subsonic flow (ref. 16)

$$R_x(\xi) = e^{-\tau_1|\xi| - \tau_2\xi}$$

$$R_y(\eta) = e^{-\tau_3|\eta|}$$

where

$$\tau_1 = \begin{cases} 0.1\,\dfrac{\omega}{U_c} & \left(\dfrac{\omega\delta^*}{U_c} \geq 0.37\right) \\[2ex] \dfrac{0.037}{\delta^*} & \left(\dfrac{\omega\delta^*}{U_c} < 0.37\right) \end{cases}$$

$$\tau_2 = i\,\frac{\omega}{U_c}$$

$$\tau_3 = 0.715\,\frac{\omega}{U_c}$$

$$U_c = \left(0.59 + 0.3e^{-0.89\omega\delta^*/U_c}\right)U_\infty$$

and U_∞ denotes the free-stream velocity; δ^*, the boundary-layer thickness. The external pressure spectral density from reference 16 is

$$\hat{S}^e(\omega) = \frac{\delta^* q_\infty^2}{U_\infty}\left(0.044e^{-0.0578\omega\delta^*/U_\infty} + 0.075e^{-0.243\omega\delta^*/U_\infty} - 0.093e^{-1.12\omega\delta^*/U_\infty}\right.$$

$$\left. - 0.025e^{-11.57\omega\delta^*/U_\infty}\right)$$

where q_∞ is free-stream dynamic pressure. For a simply supported panel with $x_0 = 0$, $\ell_x = a$, and $\ell_y = b$, $S_{mns\ell}$ can be expressed as

$$S_{mns\ell} = \frac{\hat{S}^e(\omega)}{\rho_s{}^2h^2}\,I_xI_y$$

where

$$I_x = \left[\frac{\tau_1 + \tau_2}{(\tau_1 + \tau_2)^2 + \left(\frac{s\pi}{a}\right)^2} + \frac{\tau_1 - \tau_2}{(\tau_1 - \tau_2)^2 + \left(\frac{m\pi}{a}\right)^2}\right]\delta_{ms} + \frac{2}{a}\left\{\frac{\frac{m\pi}{a}\,\frac{s\pi}{a}\left[(-1)^{m+s} - 1\right]}{\left[(\tau_1 + \tau_2)^2 + \left(\frac{m\pi}{a}\right)^2\right]\left[\left(\frac{s\pi}{a}\right)^2 - \left(\frac{m\pi}{a}\right)^2\right]}\right.$$

$$\left. + \frac{\frac{m\pi}{a}\,\frac{s\pi}{a}\left[(-1)^{m+s} - 1\right]}{\left[(\tau_1 - \tau_2)^2 + \left(\frac{s\pi}{a}\right)^2\right]\left[\left(\frac{m\pi}{a}\right)^2 - \left(\frac{s\pi}{a}\right)^2\right]}\right\}\varepsilon_{ms} + \frac{2}{a}\,\frac{\frac{m\pi}{a}\,\frac{s\pi}{a}\left[1 - (-1)^m e^{-(\tau_1-\tau_2)a}\right]}{\left[(\tau_1 - \tau_2)^2 + \left(\frac{m\pi}{a}\right)^2\right]\left[(\tau_1 - \tau_2)^2 + \left(\frac{s\pi}{a}\right)^2\right]}$$

$$+ \frac{2}{a}\,\frac{\frac{m\pi}{a}\,\frac{s\pi}{a}\left[1 - (-1)^s e^{-(\tau_1+\tau_2)a}\right]}{\left[(\tau_1 + \tau_2)^2 + \left(\frac{m\pi}{a}\right)^2\right]\left[(\tau_1 + \tau_2)^2 + \left(\frac{s\pi}{a}\right)^2\right]}$$

APPENDIX B

$$I_y = \frac{2\tau_3}{\tau_3^2 + \left(\frac{n\pi}{b}\right)^2}\,\delta_{n\ell} + \frac{2}{b}\,\frac{\frac{n\pi}{b}\,\frac{\ell\pi}{b}\left[(-1)^{n+\ell} - 1\right]}{\left[\tau_3^2 + \left(\frac{n\pi}{b}\right)^2\right]\left[\tau_3^2 + \left(\frac{\ell\pi}{b}\right)^2\right]}\,\varepsilon_{n\ell}$$

$$+ \frac{2}{b}\,\frac{\frac{n\pi}{b}\,\frac{\ell\pi}{b}\left[2 - (-1)^n e^{-\tau_3 b} - (-1)^\ell e^{-\tau_3 b}\right]}{\left[\tau_3^2 + \left(\frac{n\pi}{b}\right)^2\right]\left[\tau_3^2 + \left(\frac{\ell\pi}{b}\right)^2\right]}$$

$$\delta_{n\ell} = \begin{cases} 1 & (n = \ell) \\ 0 & (n \neq \ell) \end{cases}$$

and

$$\varepsilon_{n\ell} = \begin{cases} 0 & (n = \ell) \\ 1 & (n \neq \ell) \end{cases}$$

REFERENCES

1. Catherines, John J.; and Jha, Sunil K.: Sources and Characteristics of Interior Noise in General Aviation Aircraft. NASA TM X-72839, 1976.

2. Metzger, Frederick B.; Magliozzi, Bernard; and Pegg, Robert J.: Progress Report on Propeller Aircraft Flyover Noise Research. [Preprint] 760454, Soc. Automot. Eng., Apr. 1976.

3. Mixson, J. S.; Barton, C. K.; and Vaicaitis, R.: Interior Noise Analysis and Control for Light Aircraft. SAE Paper 770445, Mar.-Apr. 1977.

4. Lyon, Richard H.: Noise Reduction of Rectangular Enclosures With One Flexible Wall. J. Acoust. Soc. America, vol. 35, no. 11, Nov. 1963, pp. 1791-1797.

5. Pretlove, A. J.: Free Vibrations of a Rectangular Panel Backed by a Closed Rectangular Cavity. J. Sound & Vib., vol. 2, no. 3, July 1965, pp. 197-209.

6. Pretlove, A. J.: Forced Vibrations of a Rectangular Panel Backed by a Closed Rectangular Cavity. J. Sound & Vib., vol. 3, no. 3, May 1966, pp. 252-261.

7. Kihlman, T.: Sound Radiation Into a Rectangular Room. Applications to Airborne Sound Transmission in Buildings. Acustica, vol. 18, no. 1, 1967, pp. 11-20.

8. Strawderman, Wayne A.: The Acoustic Field in a Closed Space Behind a Rectangular Simply Supported Plate Excited by Boundary Layer Turbulence. USL Rep. No. 827, U.S. Navy, May 11, 1967. (Available from DDC as AD 653 455.)

9. Bhattacharya, M. C.; and Crocker, M. J.: Forced Vibration of a Panel and Radiation of Sound Into a Room. Acustica, vol. 22, no. 5, 1970, pp. 275-294.

10. Guy, R. W.; and Pretlove, A. J.: Cavity-Backed Panel Response. J. Sound & Vib., vol. 27, no. 1, Mar. 1973, pp. 128-129.

11. Guy, R. W.; and Bhattacharya, M. C.: The Transmissions of Sound Through a Cavity-Backed Finite Plate. J. Sound & Vib., vol. 27, no. 2, Mar. 1973, pp. 207-223.

12. Gorman, George F., III: An Experimental Investigation of Sound Transmission Through a Flexible Panel Into a Closed Cavity. AMS Rep. No. 924, Princeton Univ., July 1970.

13. Gorman, George F., III: Random Excitation of a Panel-Cavity System. AMS Rep. No. 1009 (NASA Grant NGR 31-001-146), Princeton Univ., July 1971. (Also available as NASA CR-112051.)

14. Dowell, E. H.: Acoustoelasticity. NASA CR-145110, 1977.

15. Priestley, M. B.: Evolutionary Spectra and Non-Stationary Processes. J. Roy. Statist. Soc., ser. B, vol. 27, 1965, pp. 204-237.

16. Lin, Y. K.: Probabilistic Theory of Structural Dynamics. McGraw-Hill Book Co., Inc., c.1967.

17. Chyu, Wei J.; and Au-Yang, M. K.: Random Response of Rectangular Panels to the Pressure Field Beneath a Turbulent Boundary Layer in Subsonic Flows. NASA TN D-6970, 1972.

18. Dowell, E. H.; and Vaicaitis, R.: A Primer for Structural Response to Random Pressure Fluctuations. AMS Rep. No. 1220 (NASA Grants NGR 31-001-146 and NSG 1059), Princeton Univ., April 1975. (Also available as NASA CR-142671.)

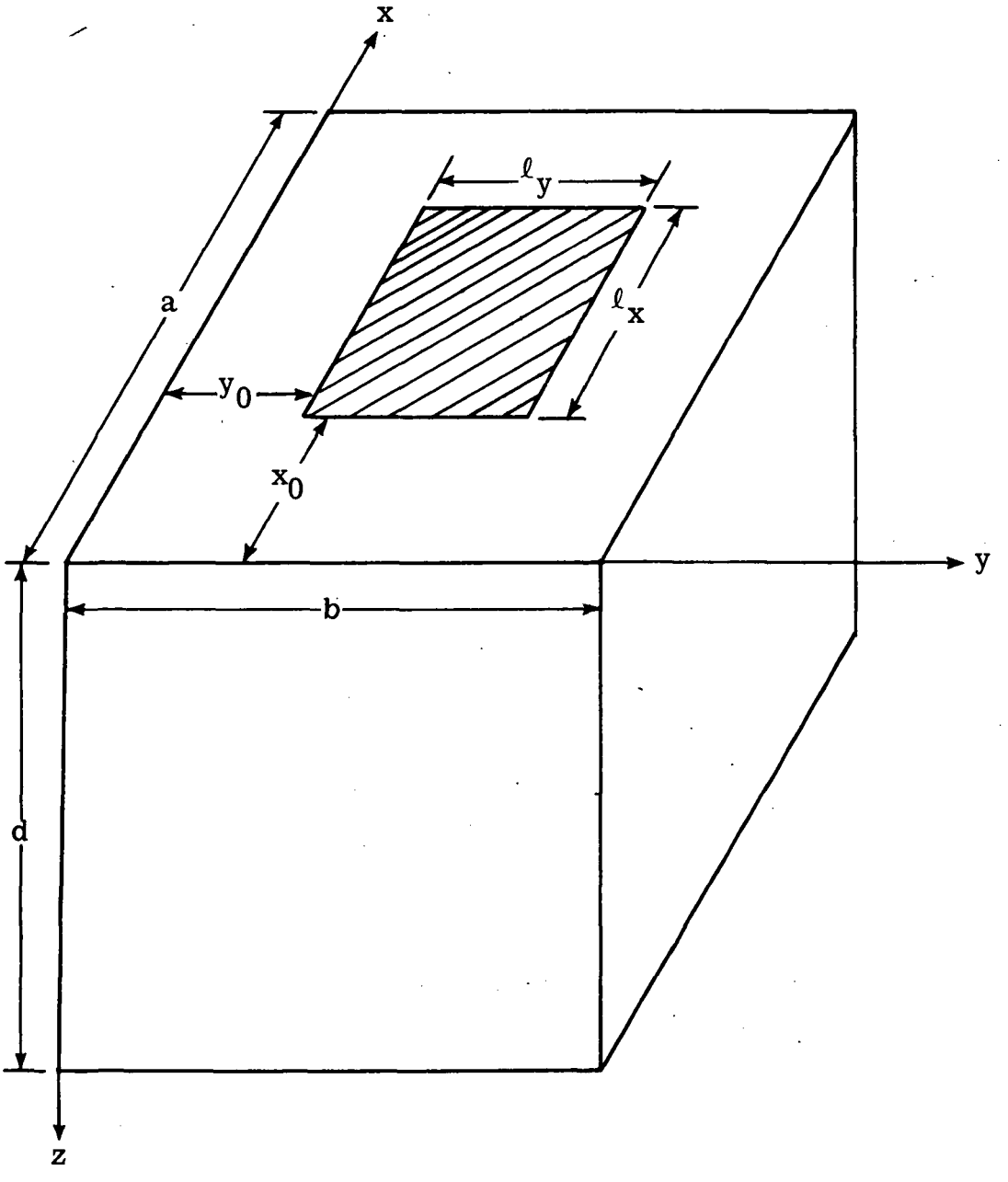

Figure 1.- Cavity and panel geometry.

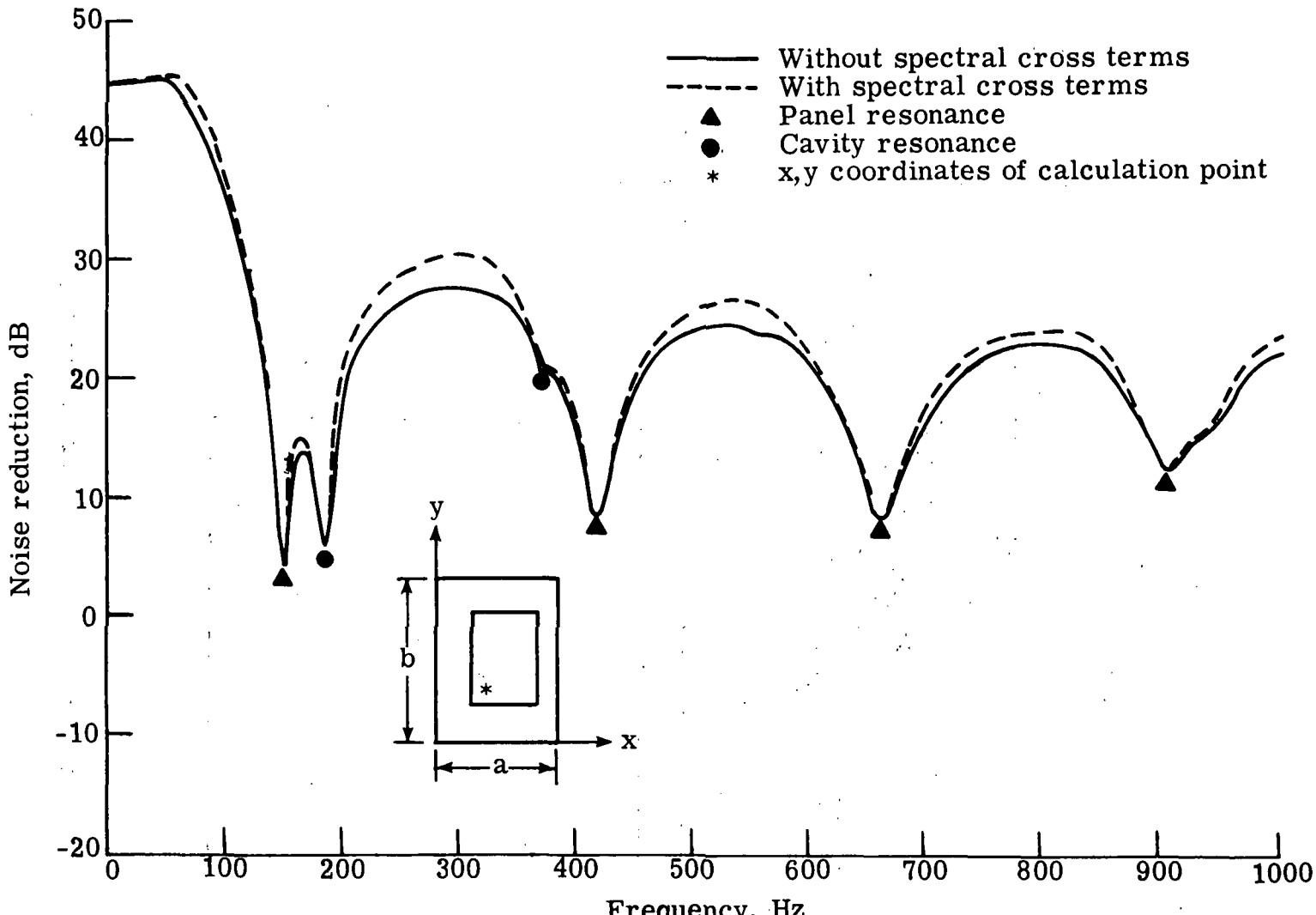

Figure 2.- Contribution of spectral cross terms in calculation of noise reduction for a clamped panel.

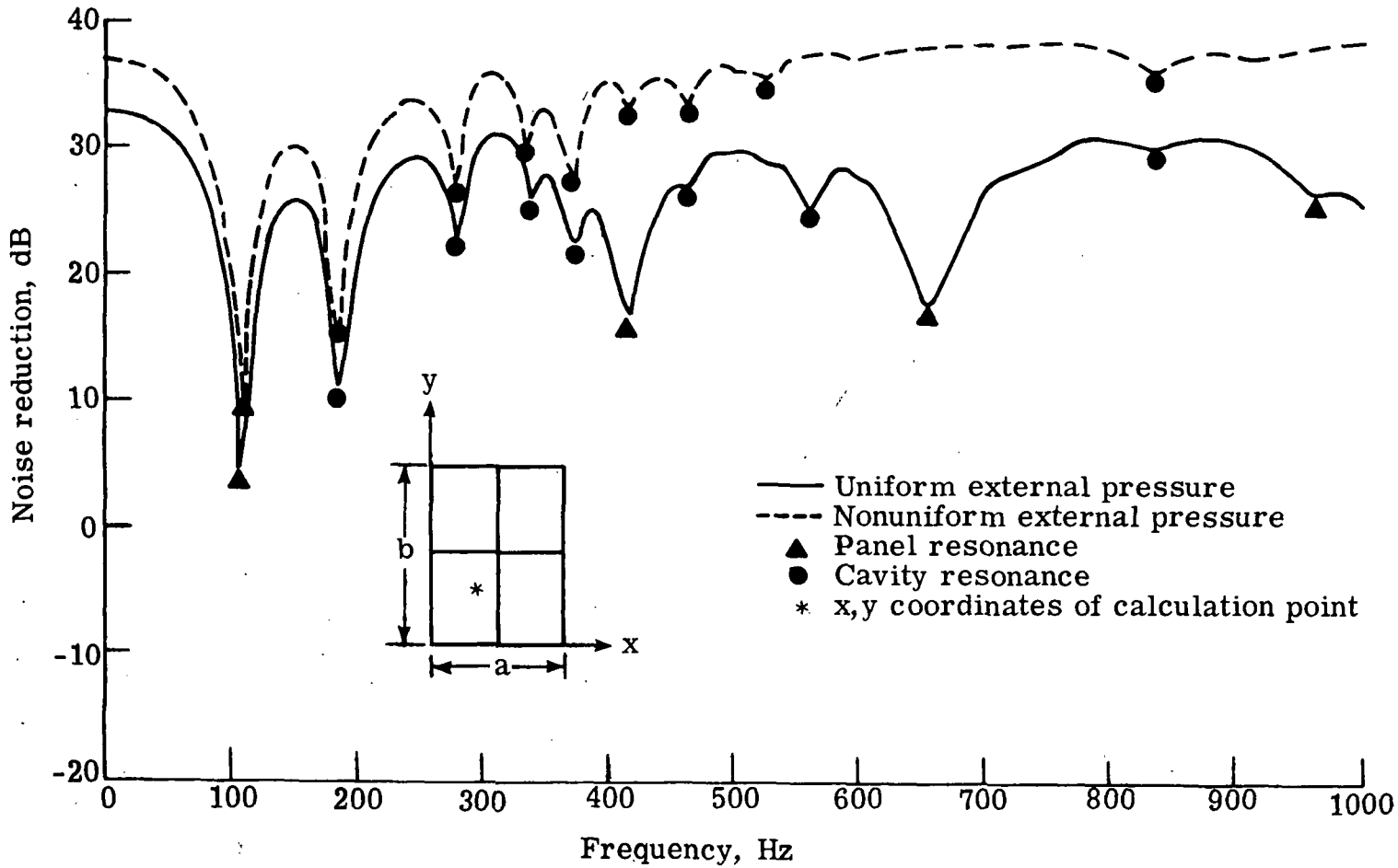

Figure 3.- Noise reduction for uniform and nonuniform external pressure distributions for a wall composed of four equal size simply supported panels.

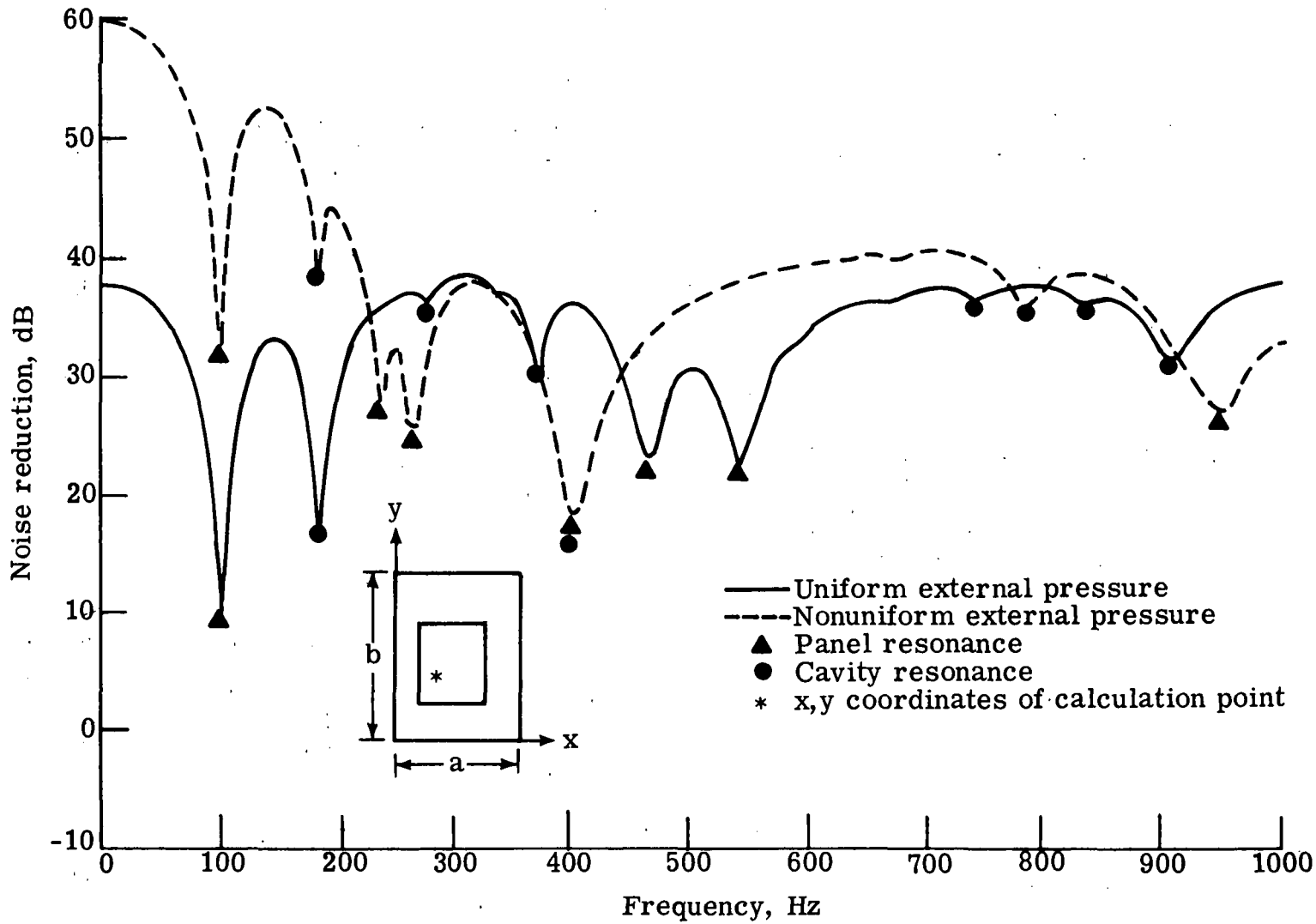

Figure 4.- Noise reduction for uniform and nonuniform external pressure distributions for a single simply supported panel.

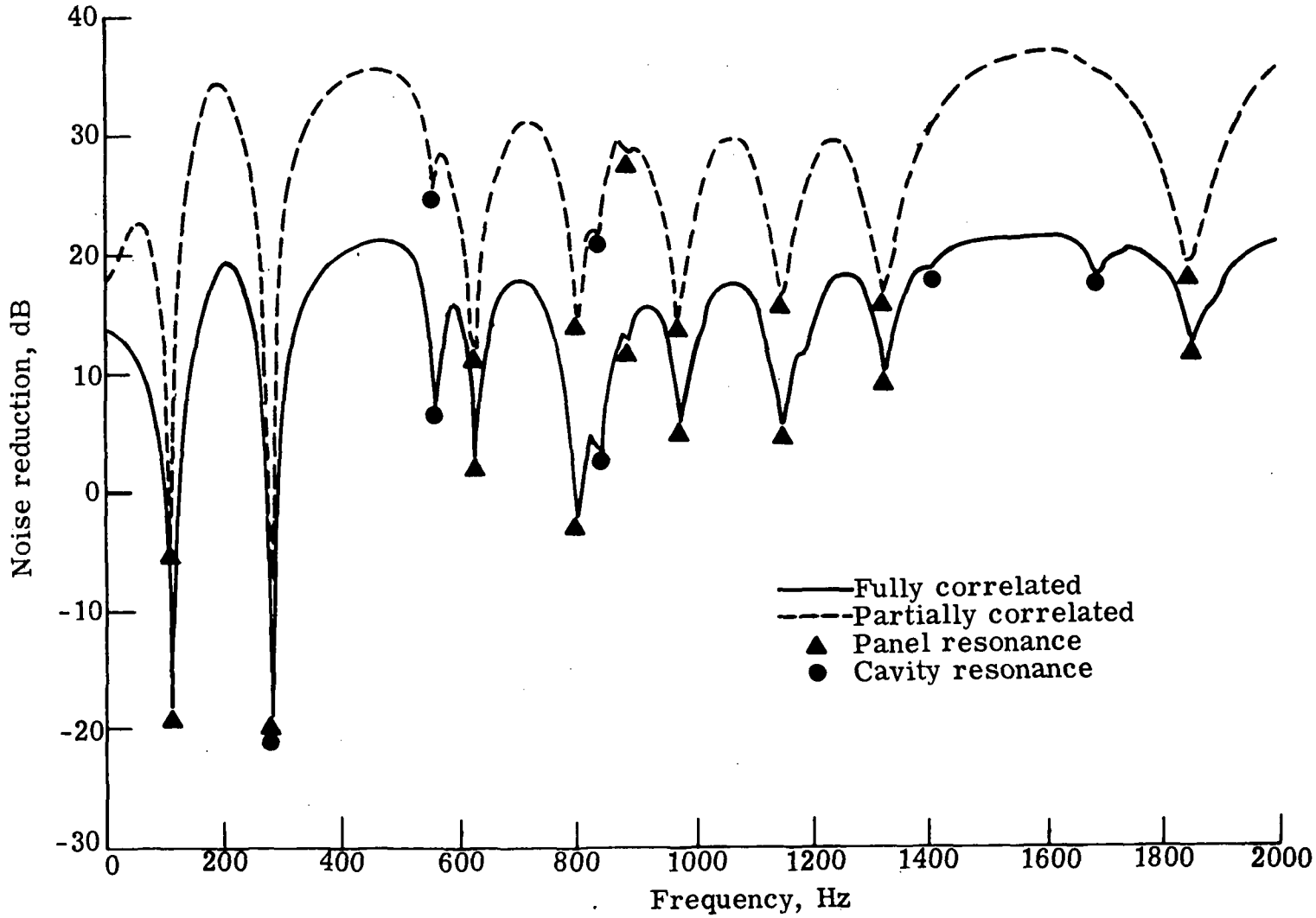

Figure 5.- Noise reduction for fully correlated and partially correlated turbulent boundary-layer noise over a simply supported panel.

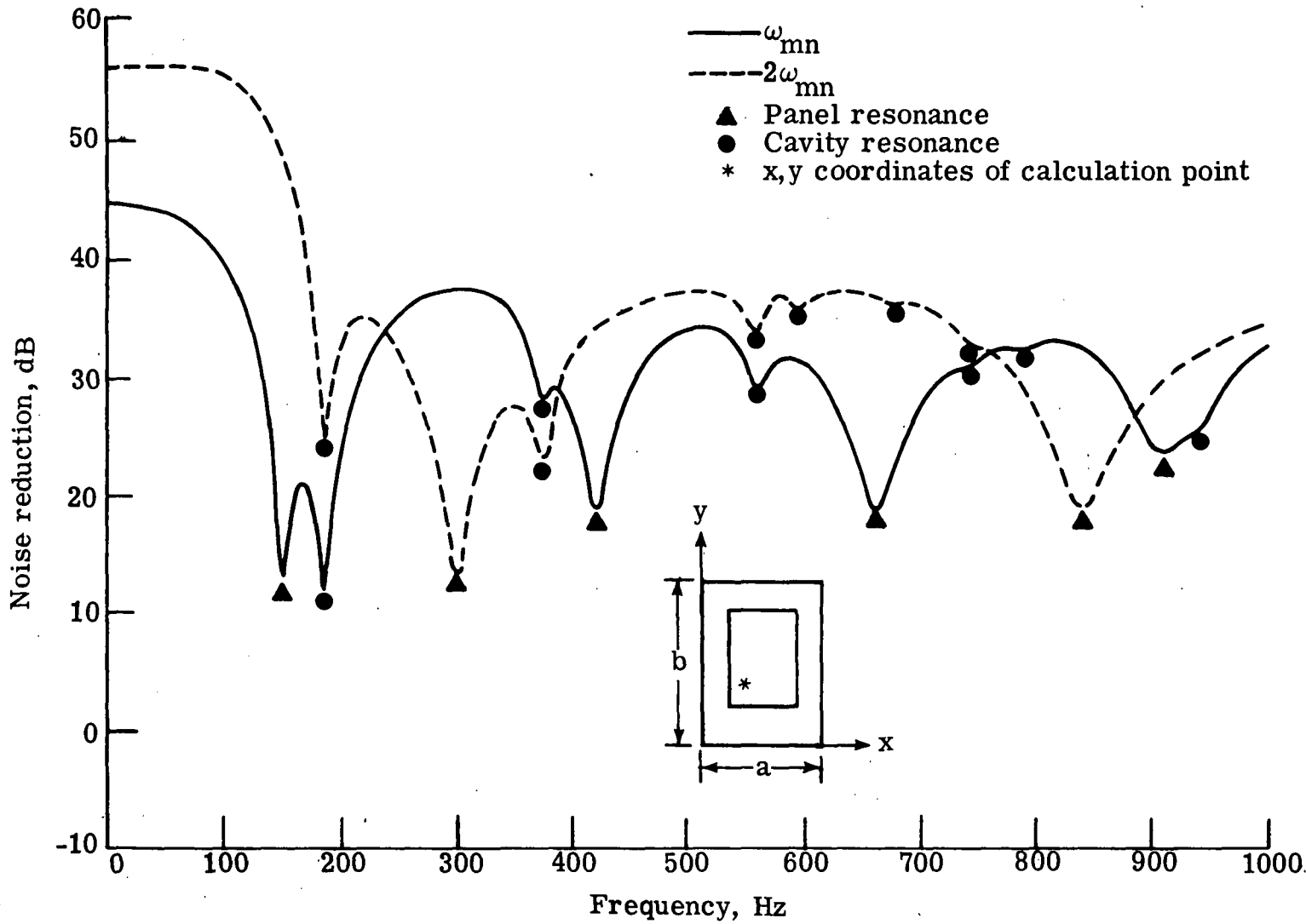

Figure 6.- Effect on noise reduction of doubling panel natural frequencies. Clamped panel; spatially uniform external pressure.

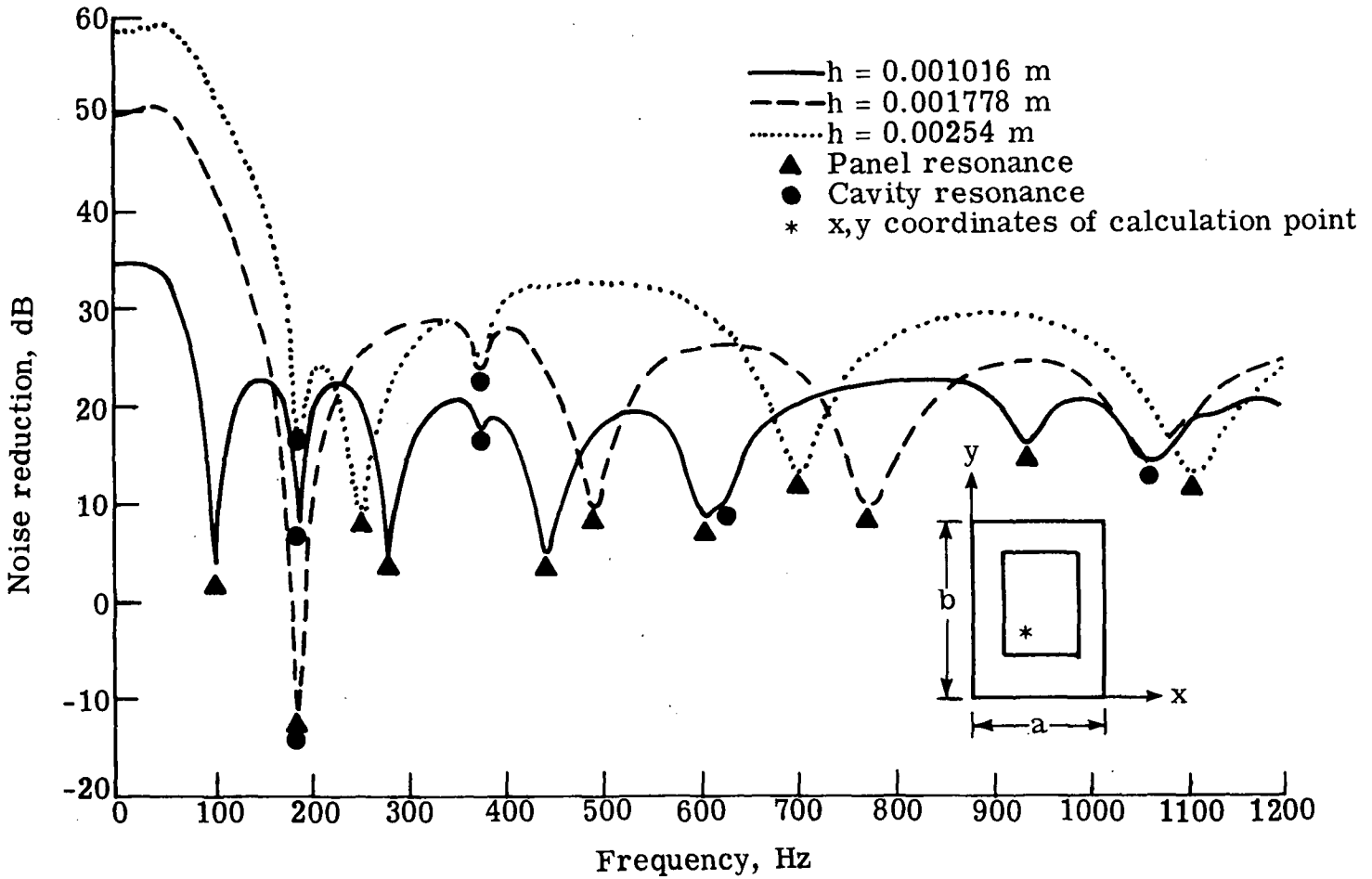

Figure 7.- Effect of panel thickness on noise reduction. Clamped panel; spatially uniform external pressure.

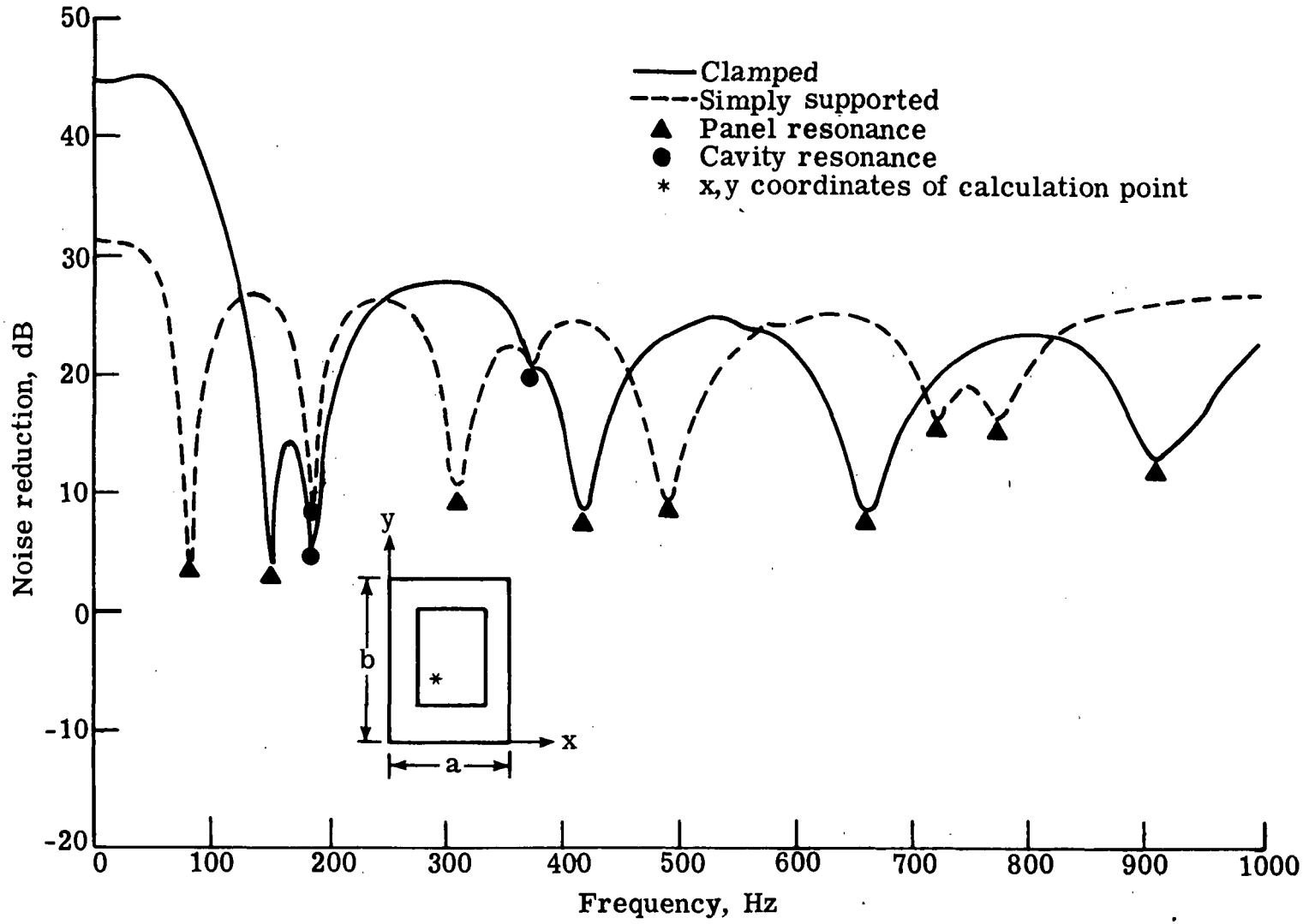

Figure 8.- Comparison of noise reduction for clamped and simply supported panels. Uniform external pressure.

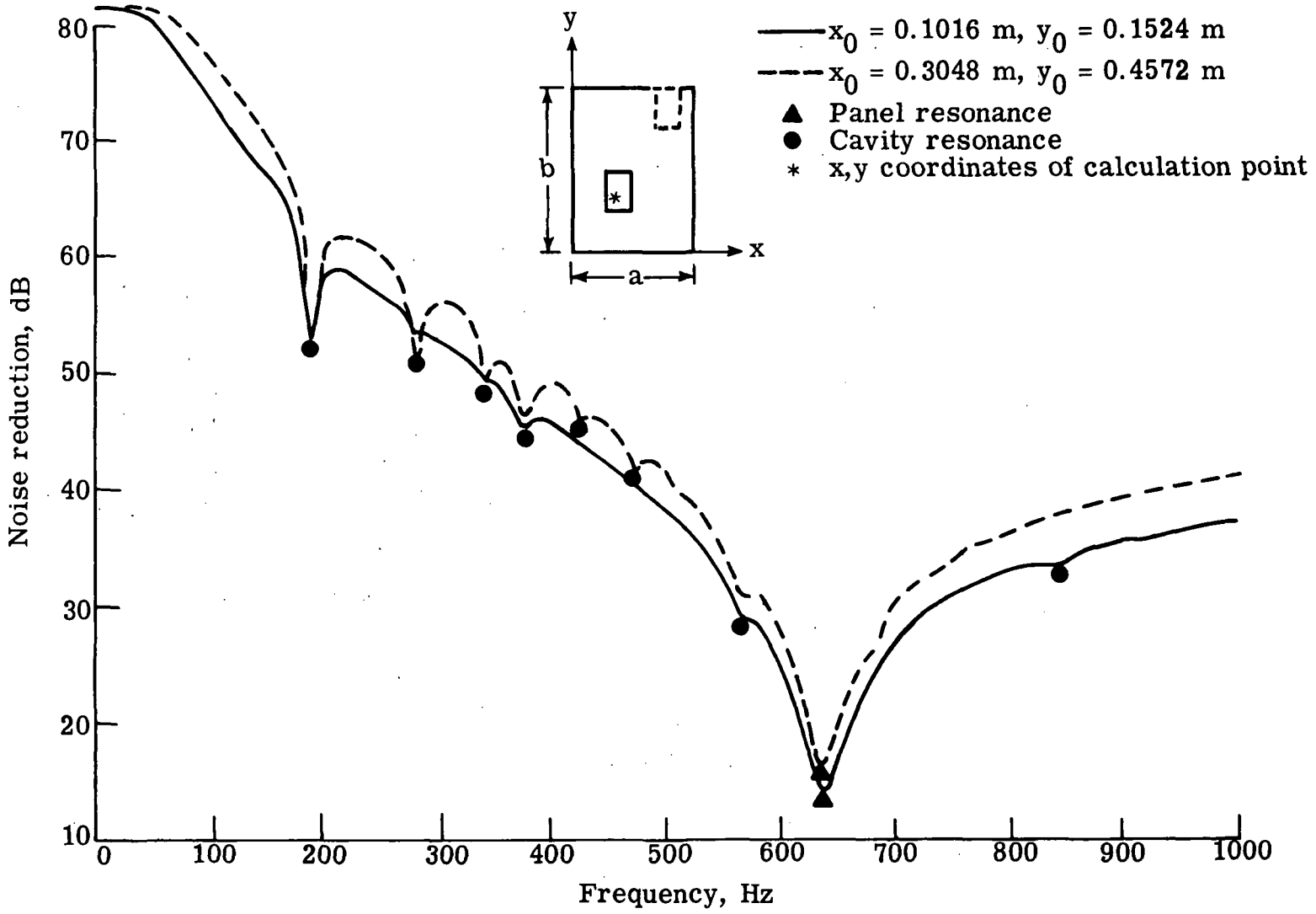

Figure 9.- Effect on noise reduction of panel position on wall. Clamped panel; uniform external pressure.

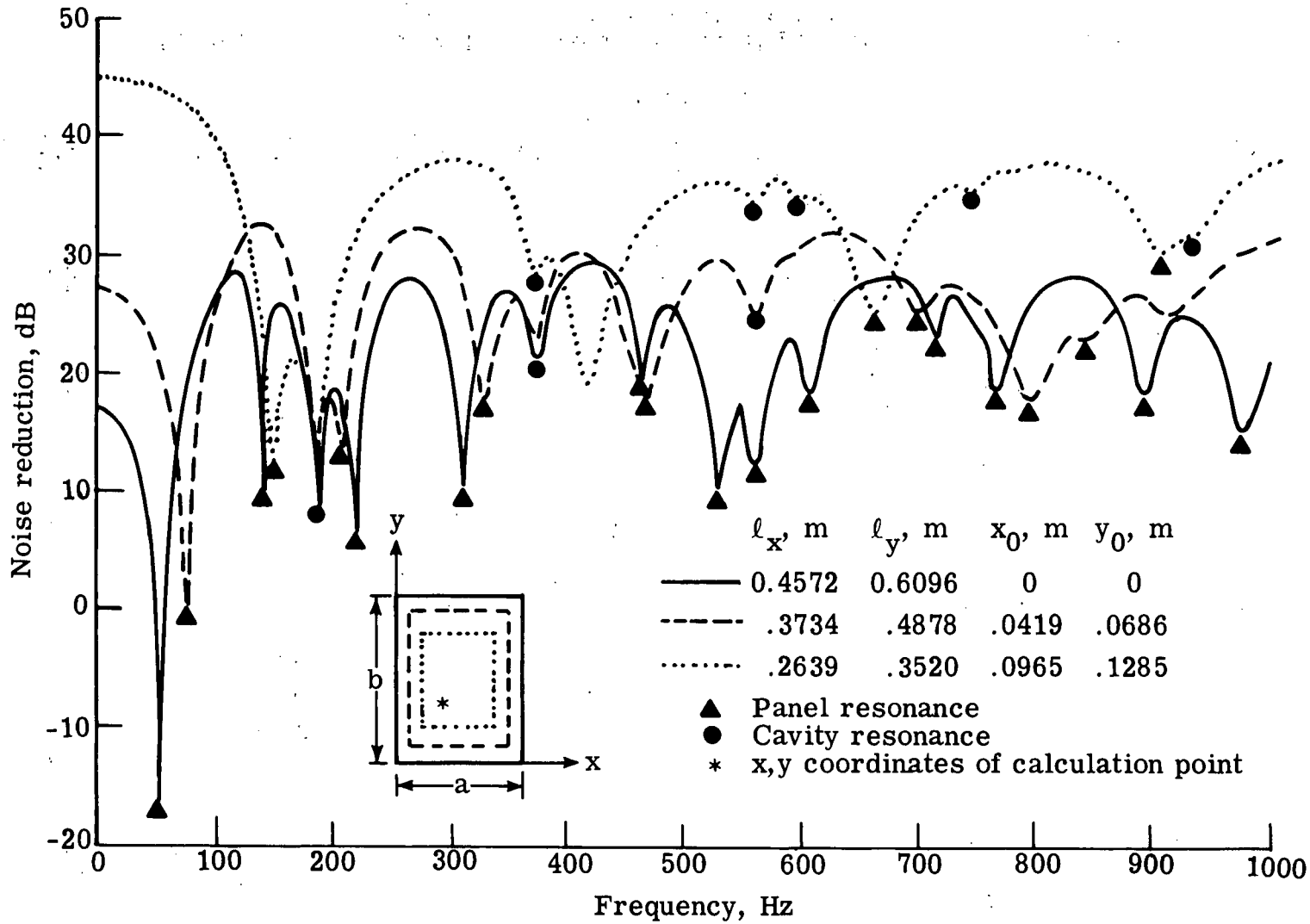

Figure 10.- Effect of panel size on noise reduction. Clamped panel; uniform external pressure.

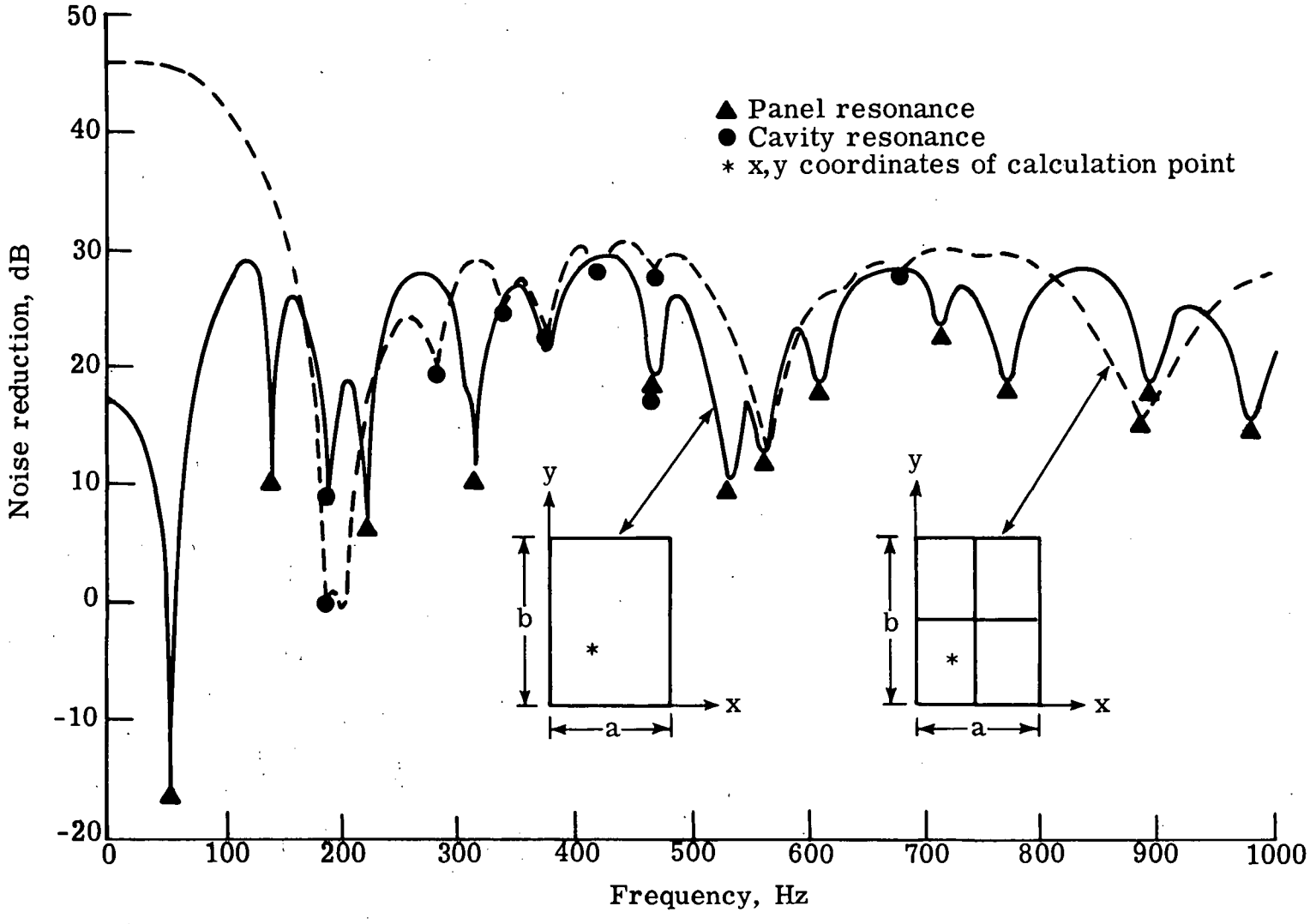

Figure 11.- Comparison of noise reduction for four equal size panels and a single panel. Clamped panels; uniform external pressure.

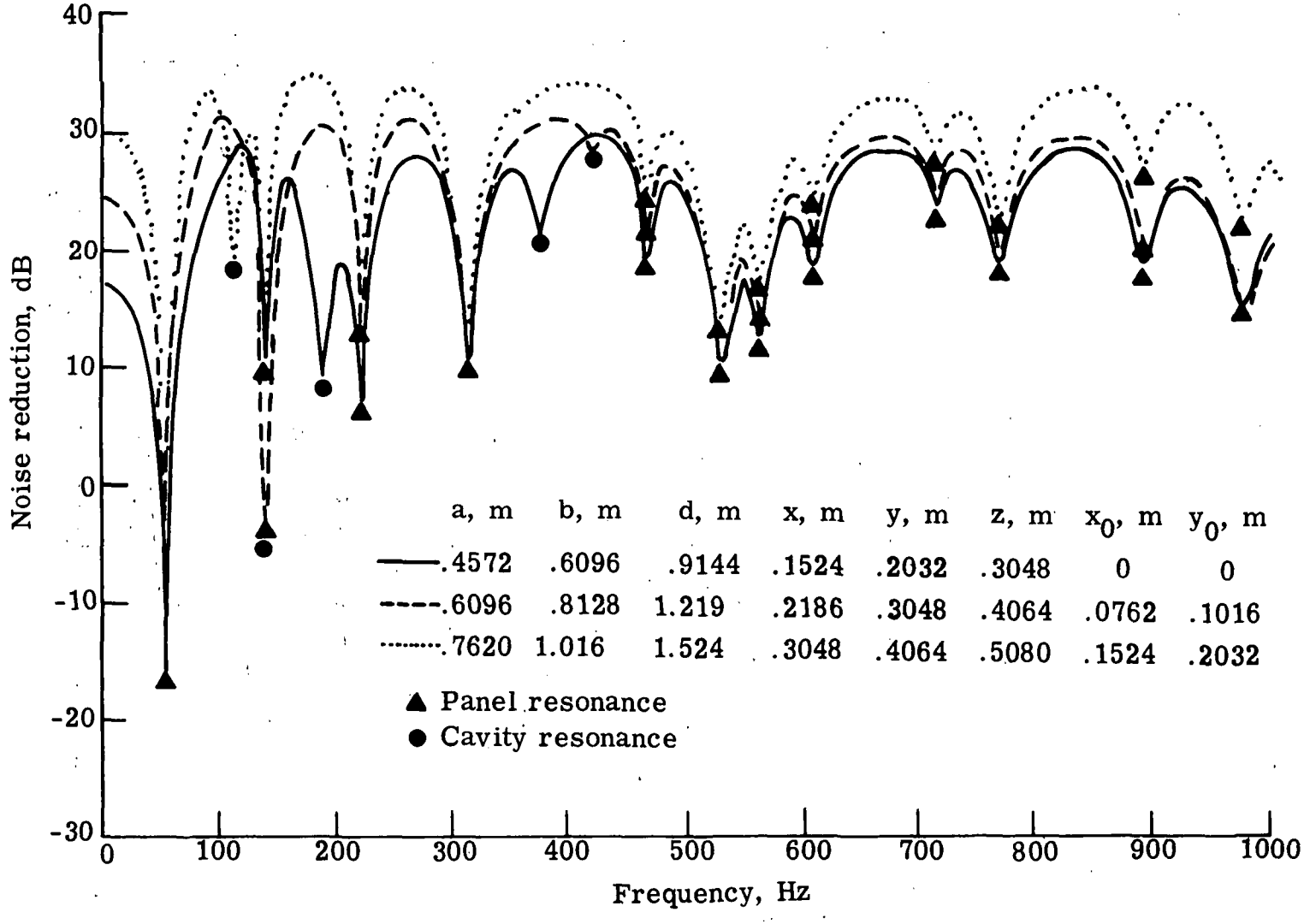

Figure 12.- Effect of cavity size on noise reduction.

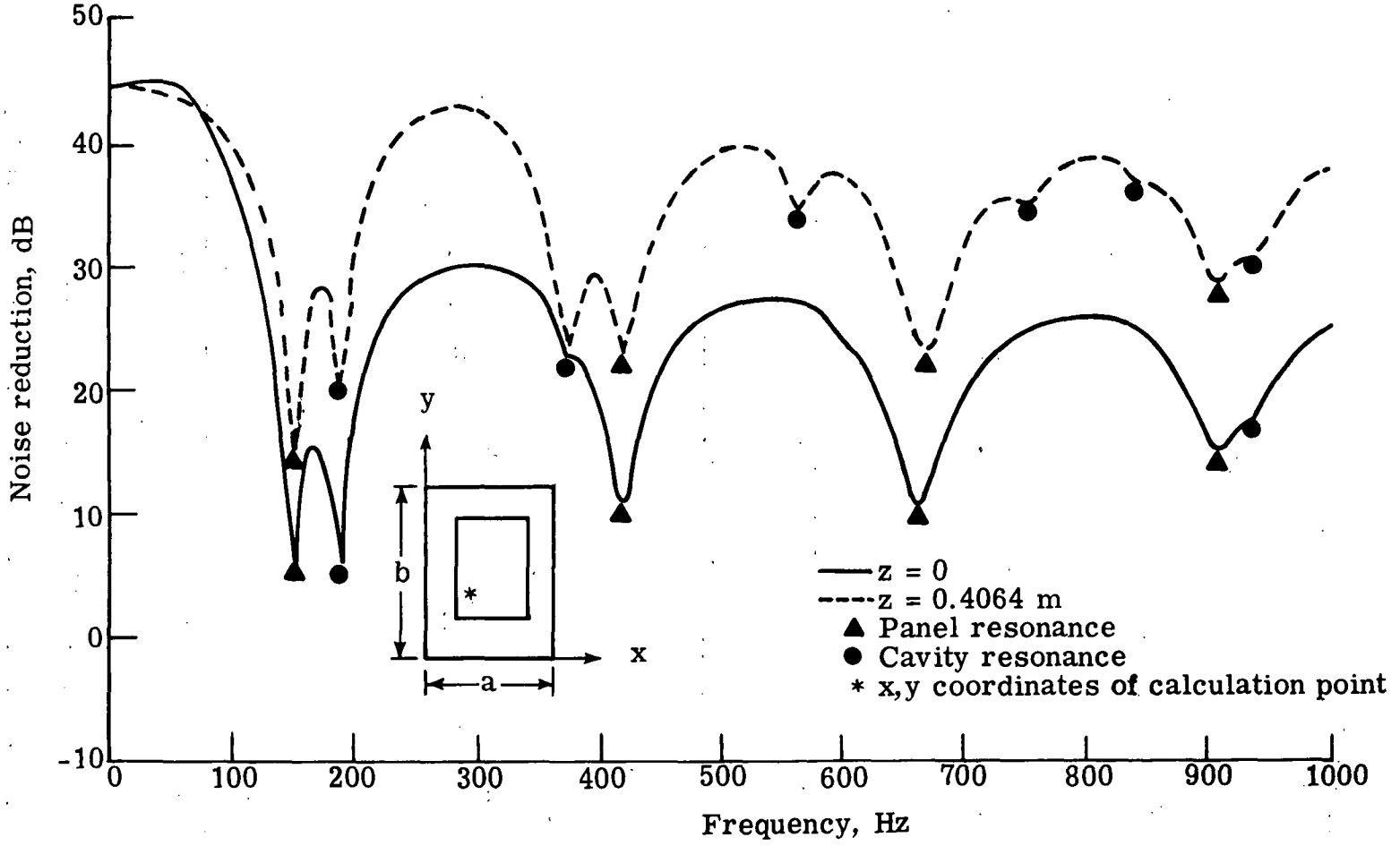

Figure 13.- Noise reduction at two different distances below panel.

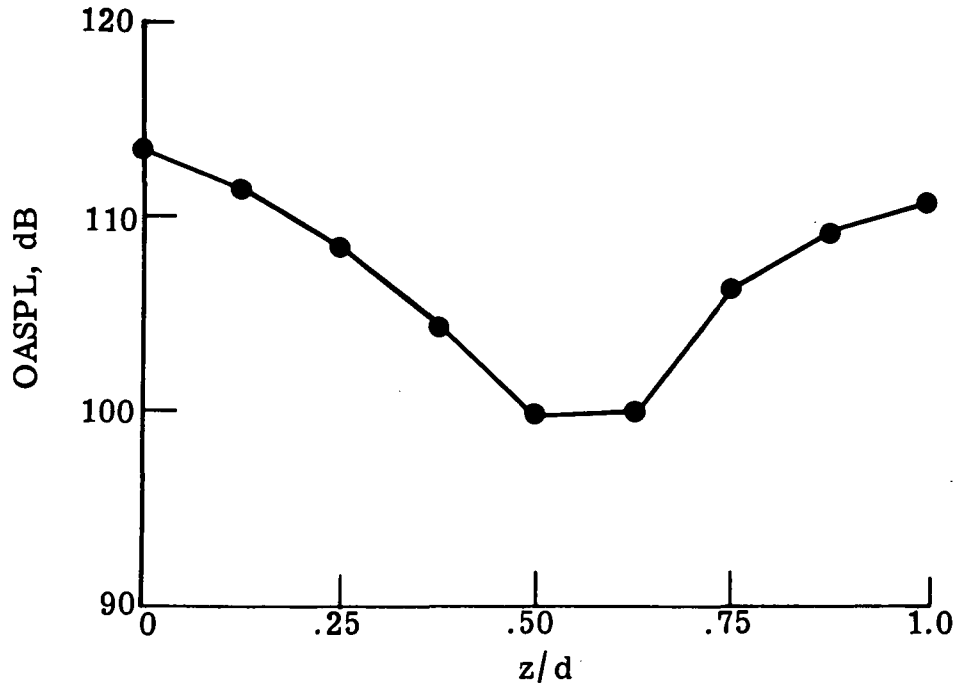

(a) Variation with distance below plate.

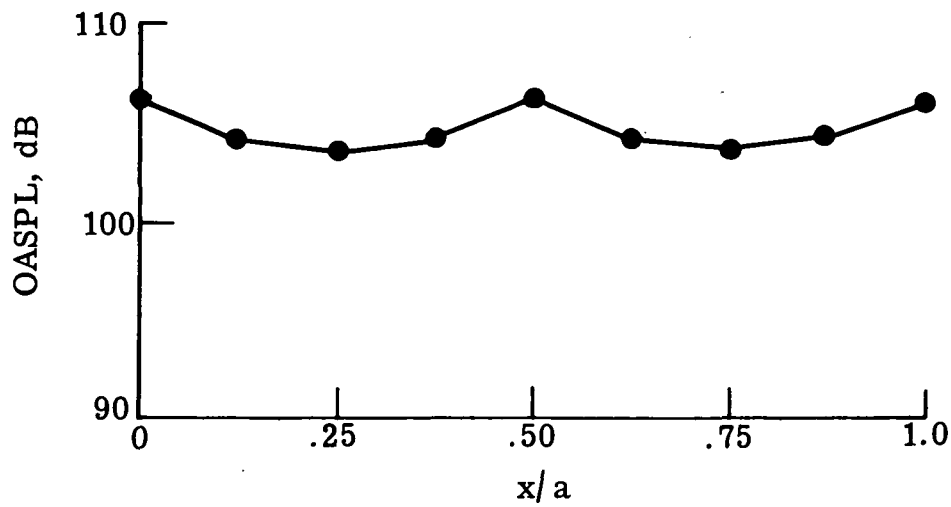

(b) Variation parallel to plate.

Figure 14.- Variation of OASPL with position in cavity.

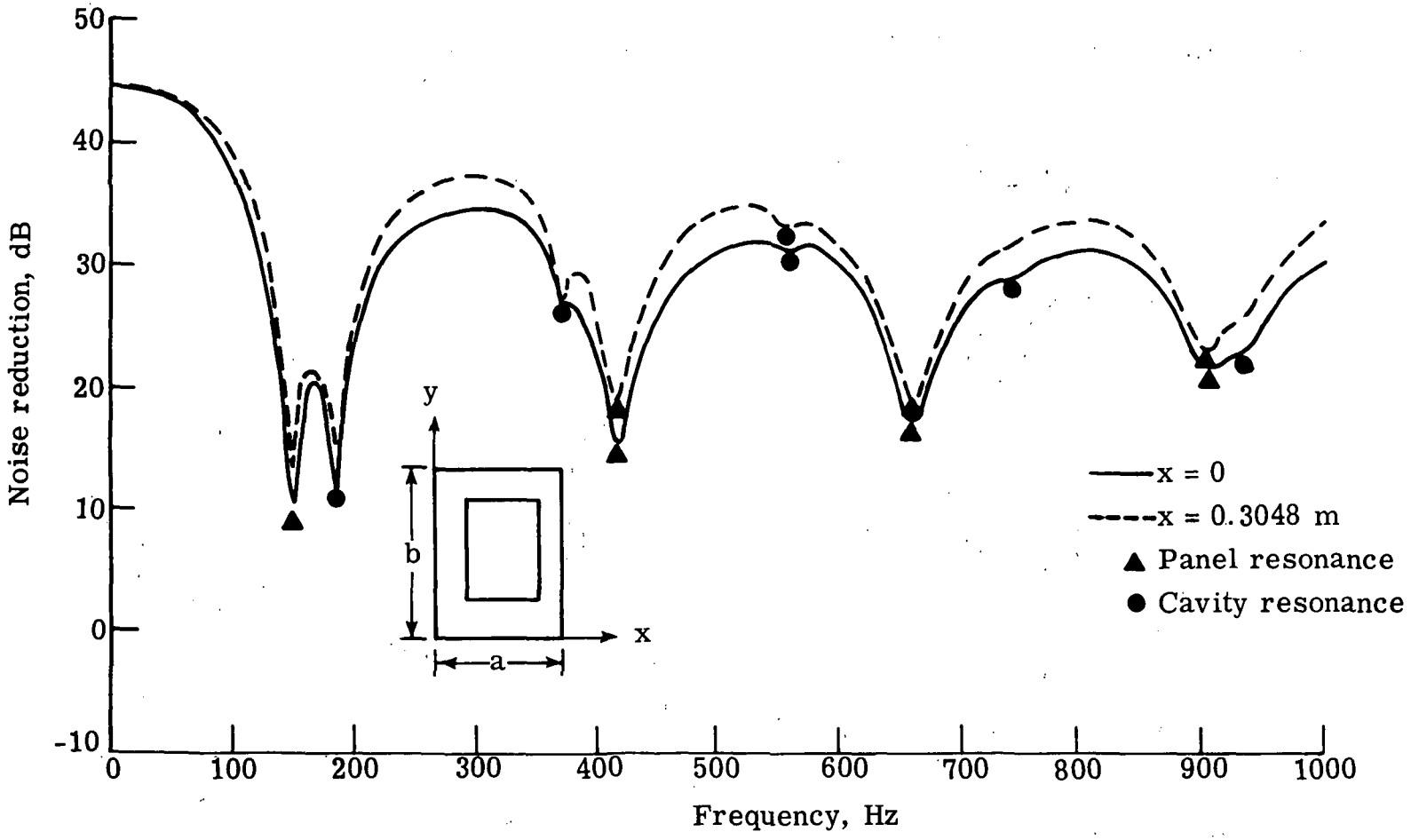

Figure 15.- Noise reduction at two different values of x.

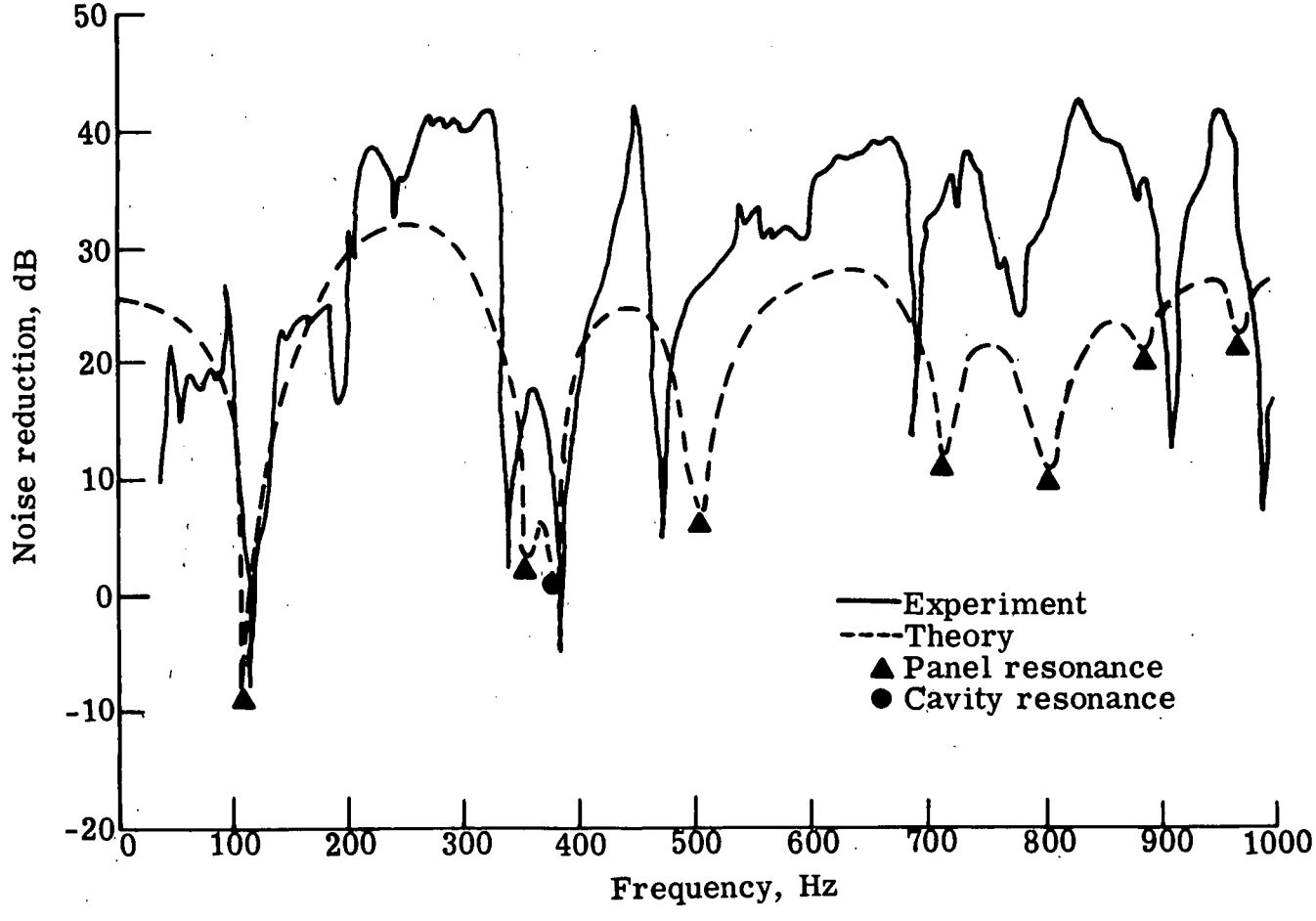

Figure 16.- Theoretical and experimental narrow band spectrum of noise reduction.

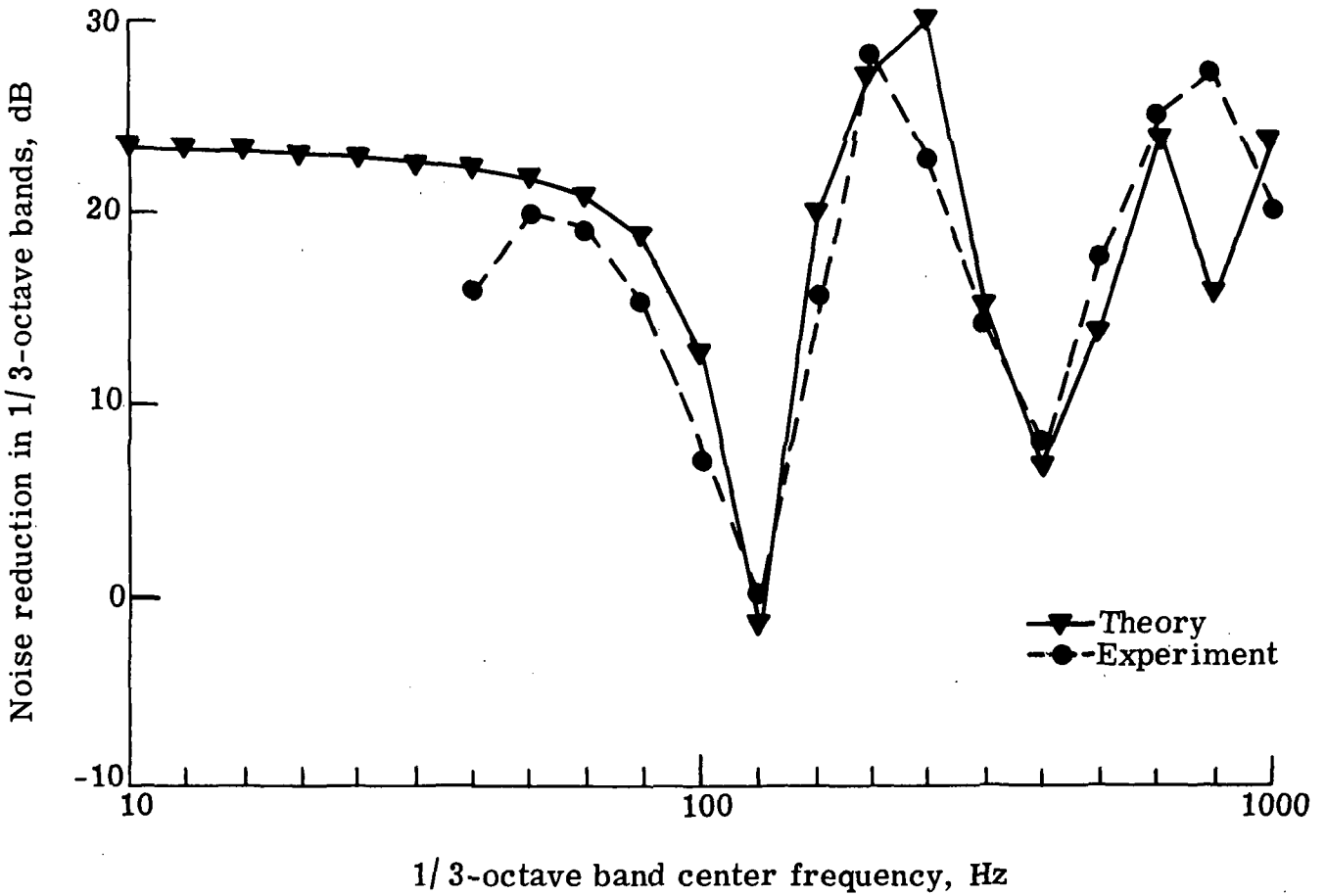

Figure 17.- Theoretical and experimental 1/3-octave band spectrum of noise reduction.

1. Report No.	2. Government Accession No.	3. Recipient's Catalog No.
NASA TP-1173		

4. Title and Subtitle	5. Report Date
NOISE TRANSMISSION THROUGH PLATES INTO AN ENCLOSURE	May 1978
	6. Performing Organization Code
7. Author(s)	8. Performing Organization Report No.
Wayne B. McDonald, Rimas Vaicaitis, and Michael K. Myers	L-11906
9. Performing Organization Name and Address	10. Work Unit No.
NASA Langley Research Center Hampton, VA 23665	505-09-23-01
	11. Contract or Grant No.
12. Sponsoring Agency Name and Address	13. Type of Report and Period Covered
National Aeronautics and Space Administration Washington, DC 20546	Technical Paper
	14. Sponsoring Agency Code

15. Supplementary Notes

Wayne B. McDonald and Michael K. Myers: The George Washington University, Joint Institute for Advancement of Flight Sciences.

Rimas Vaicaitis: Columbia University; completed a 1-year appointment at Langley Research Center in July 1977 under the Intergovernmental Personnel Act of 1970.

The contribution of Wayne B. McDonald to this report was performed as part of the requirements for the degree of Master of Science, The George Washington University, Washington, D.C.

16. Abstract

An analytical model is presented to predict noise transmission through elastic plates into a hard-walled rectangular cavity at low frequencies, that is, frequencies up through the first few plate and cavity natural frequencies. One or several nonoverlapping and independently vibrating panels are considered. The effects on noise transmission of different external-pressure excitations, plate boundary conditions, fluid parameters, structural parameters, and geometrical parameters are investigated.

17. Key Words (Suggested by Author(s))	18. Distribution Statement
Acoustics Noise transmission Random vibrations Rectangular plates	Unclassified - Unlimited Subject Category 71

19. Security Classif. (of this report)	20. Security Classif. (of this page)	21. No. of Pages	22. Price*
Unclassified	Unclassified	43	$4.50

* For sale by the National Technical Information Service, Springfield, Virginia 22161

NASA-Langley, 1978

National Aeronautics and
Space Administration

Washington, D.C.
20546

Official Business
Penalty for Private Use, $300

THIRD-CLASS BULK RATE

Postage and Fees Paid
National Aeronautics and
Space Administration
NASA-451

U.S.MAIL

NASA

POSTMASTER: If Undeliverable (Section 158 Postal Manual) Do Not Return